การเตรียมท่อนาโนพอลิแอนิลีนที่จัดเรียงตัวเองสำหรับการขจัดนิกเกิล (II)

นางสาวศิรินันท์ ขุนฤทธิ์

วิทยานิพนธ์นี้เป็นส่วนหนึ่งของการศึกษาตามหลักสูตรปริญญาวิทยาศาสตรมหาบัณฑิต
สาขาวิชาปิโตรเคมีและวิทยาศาสตร์พอลิเมอร์
คณะวิทยาศาสตร์ จุฬาลงกรณ์มหาวิทยาลัย
ปีการศึกษา 2555

PREPARATION OF SELF-ASSEMBLED POLYANILINE NANOTUBES FOR REMOVAL OF NICKEL(II)

Miss Sirinan Khunrit

A Thesis Submitted in Partial Fulfillment of the Requirements
for the Degree of Master of Science Program in Petrochemistry and Polymer Science
Faculty of Science
Chulalongkorn University
Academic Year 2012

Thesis Title	PREPARATION OF SELF-ASSEMBLED POLYANILINE NANOTUBES FOR REMOVAL OF NICKEL(II)
By	Miss Sirinan Khunrit
Field of Study	Petrochemistry and Polymer Science
Thesis Advisor	Puttaruksa Varanusupakul, Ph.D.

Accepted by the Faculty of Science, Chulalongkorn University in Partial Fulfillment of the Requirements for the Master's Degree

……………………………………….. Dean of the Faculty of Science
(Professor Supot Hannongbua, Dr.rer.nat.)

THESIS COMMITTEE

…………………………………….…. Chairman
(Assistant Professor Warinthorn Chavasiri, Ph.D.)

……………………………………….. Thesis Advisor
(Puttaruksa Varanusupakul, Ph.D.)

…………………………………….…. Examiner
(Amarawan Intasiri, Ph.D.)

……………………………..….….…. External Examiner
(Pongphisanu Muangchareon, Ph.D.)

ศิรินันท์ ขุนฤทธิ์: การเตรียมท่อนาโนพอลิแอนิลีนที่จัดเรียงตัวเองสำหรับการขจัดนิกเกิล (II). (PREPARATION OF SELF-ASSEMBLED POLYANILINE NANOTUBES FOR REMOVAL OF NICKEL(II)) อ.ที่ปรึกษาวิทยานิพนธ์หลัก: อ.ดร.พุทธรักษา วรานุศุภากุล, 62 หน้า.

ในงานวิจัยนี้ได้เตรียมท่อนาโนพอลิแอนิลีนที่จัดเรียงตัวเองสำหรับการขจัดนิกเกิล (II) ทำการศึกษาปัจจัยในการสังเคราะห์ท่อนาโนพอลิแอนิลีนที่มีผลต่อลักษณะโครงสร้างสัณฐานของท่อนาโนคือ ชนิดของกรดอินทรีย์ที่ใช้เป็นตัวโดป อีกทั้งศึกษาผลของการเติมเมทานอลและผลของอัตราส่วนโดยโมลของแอนิลีนมอนอเมอร์กับตัวโดป พบว่า เมื่อใช้ตัวโดปที่เป็นกรดอินทรีย์ขนาดเล็ก จะทำให้เกิดท่อนาโนผ่านกลไกที่ฟีนาซีนประพฤติตัวเป็นแม่แบบ และเมื่อใช้กรดอินทรีย์ที่มีส่วนที่ไม่ชอบน้ำเป็นส่วนประกอบ จะทำให้เกิดท่อนาโนผ่านกลไกไมเซลล์ประพฤติตัวเป็นแม่แบบ โดยจะทำให้ได้ขนาดเส้นผ่านศูนย์กลางภายนอกของท่อนาโนที่ใกล้เคียงกันอยู่ในช่วง 220-330 นาโนเมตร ขนาดเส้นผ่านศูนย์กลางภายในของท่อนาโนที่โดปด้วยกรด DBSA มีขนาดใหญ่กว่าการโดปด้วยกรดอินทรีย์ขนาดเล็ก แต่การโดปด้วยกรด DBSA จะพบว่ามีแท่งนาโนเกิดขึ้นมากกว่าท่อนาโน นอกจากนี้ การใช้กรดคาร์บอกซิลิกเป็นตัวโดป ทำให้ได้ท่อนาโนพอลิแอนิลีนที่เป็นรูปแบบเดียวกันมากกว่าการใช้กรดซัลโฟนิก เมื่อพิจารณาตัวโดปที่ประกอบด้วยหมู่อัลคิลและเบนซิลต่างกัน พบว่าไม่ส่งผลอย่างมีนัยสำคัญต่อโครงสร้างสัณฐานของท่อนาโนที่ได้ เมื่อมีการใช้กรดคาร์บอกซิลิกที่ประกอบด้วยหมู่ไฮดรอกซิลเป็นตัวโดป จะทำให้ได้ท่อนาโนที่เกิดการเกาะกลุ่มจนมีลักษณะเหมือนปะการัง และเมื่อทำการสังเคราะห์ท่อนาโนในสารละลายที่มีเมทานอล จะทำให้ท่อนาโนสูญเสียความเป็นรูปแบบเดียวกันและเกิดการเกาะกลุ่มกันของรูปร่างที่เป็นเม็ดกลมมากขึ้น และอัตราส่วนโดยโมลที่เหมาะสม คือ 0.2 เมื่อนำท่อนาโนพอลิแอนิลีนที่สังเคราะห์ได้ไปขจัดนิกเกิล(II) พบว่า ท่อนาโนพอลิแอนิลีนที่ใช้ตัวโดปต่างกัน จะให้ประสิทธิภาพในการขจัดนิกเกิลที่ใกล้เคียงกัน โดยเวลาที่ใช้ในการดูดซับนิกเกิลจนเข้าสู่สมดุล คือ 18 ชั่วโมง และค่า pH ของสารตัวอย่างที่เหมาะสมในการดูดซับนิกเกิลคือ 6

สาขาวิชา ปิโตรเคมีและวิทยาศาสตร์พอลิเมอร์ ลายมือชื่อนิสิต..............................

ปีการศึกษา 2555 ลายมือชื่อ อ.ที่ปรึกษาวิทยานิพนธ์หลัก..............................

537 23415 23: MAJOR PETROCHEMISTRY AND POLYMER SCIENCE
KEYWORDS: POLYANILINE/ SELF-ASEMBLY/ NANOTUBES/ HEAVY METAL REMOVAL/ NICKEL (Ni(II)) IONS

SIRINAN KHUNRIT: PREPARATION OF SELF-ASSEMBLED POLYANILINE NANOTUBES FOR REMOVAL OF NICKEL(II). ADVISOR: PUTTARUKSA VARANUSUPAKUL, Ph.D., 62 pp.

Polyaniline (PANI) nanotubes were prepared by the self-assembly method in the presence of various organic acid dopants for removal of Ni(II). The small organic acid dopants were leading to phenazine templating mechanism of self-assembled PANI nanotubes while the long hydrophobic were leading to micelles as soft template mechanism. All the nanostructures formed by doping PANI with different acids were nanotubes but nanorods and nanoparticles also co-exist. The outer diameters of obtained PANI nanotubes were in range of 220-330. The inner diameter of PANI nanotubes doped with DBSA was larger than those of PANI doped with other small organic acids. However, the nanorods were obtained much more than nanotubes when PANI nanotubes doped with DBSA. PANI nanotubes doped with carboxylic acid dopants were more uniform than those doped with sulfonic acid dopants. Moreover, alkyl and benzyl moieties contained in dopants insignificantly affected the morphology of PANI nanotubes. When the carboxylic acid dopants contain hydroxyl group, the PANI nanotubes aggregated to formed dendrites. For the additional of methanol in reaction solution, the nanotubes and nanorods became irregular and lost their uniform morphology. The uniformity of nanotubes was excellent as the molar ratio is 0.2. PANI nanotubes can be used for removal of Ni(II) ions in solution. The adsorption capacity of PANI nanotubes that doped with various dopants was similar. The suitable condition that result the maximum adsorption amount was pH 6 and contact time of 18 h.

Field of Study: Petrochemistry and Polymer Science Student's Signature.
Academic Year: 2012 Advisor's Signature.

ACKNOWLEDGEMENTS

The author thanks and appreciates many people for kindly suggestion about the knowledge in this study. First, I would like to express my heartfelt gratitude and sincere thank to my respectful advisor, Dr. Puttaruksa Varanusupakul, for consulting a good and usefulness to my research. Despite it had a lot of obstacles, the research could move forward. Thank you for kindliness, remission and patience of my slow understanding so advisor needs to repeat it. Additionally, I would like to extend my appreciation to Assistant Professor Dr. Warinthorn Chavasiri, Dr. Amarawan Intasiri and Dr. Pongphisanu Muangchareon for their valuable suggestions as my thesis committees.

I would like to thank many people in Chromatography and Separation Research Unit (ChSRU) and all the seniors who graduated in last year and present members of 1205/1207 Laboratory. Thanks for your kindliness, regards, remission, listening and suggestion for the problems about my thesis. I felt good throughout the making my thesis because all members had a funny story that made me laugh. Since we often went to eat and talk about the general story together, it made our relationship so close. I’m very glad to have the chance to known everyone.

Finally, I would like to thank my beloved family; father, mother, older sister and my intimate friends for all their love, understanding, support, counsel, encouragement and consolation.

CONTENTS

Page

Page

LIST OF TABLES

LIST OF FIGURES

Figure **Page**

LIST OF ABBREVIATIONS

ppm	Part per million
nm	Nanometer
pm	Picometer
cm	Centrimater
°C	Celcius degree
mg	Milligram
g	Gram
M	Molar concentration
s	Second
min	Minute
h	Hour
S	Siemen
mL	Milliliter
L	Liter
PANI	Polyaniline

CHAPTER I

INTRODUCTION

1.1 Motivation of proposer

Polyaniline (PANI) is one of the most useful conducting polymers due to its controllable chemical and physical properties by oxidation and protonation states, easy synthesis, excellent environmental stability, high electronic conductivity, low cost and a large variety of applications such as rechargeable batteries, gas sensor, optical devices and removal of heavy metals. A variety of chemical methods have been developed to synthesize one-dimensional PANI nanostructures [1]. The chemical approaches for production of one-dimensional PANI nanostructures are basically divided into hard and soft template (or self-template or template-free or self-assembly) synthesis. Other methods such as interfacial polymerization, electrochemical polymerization were also developed. Hard template method has been studied widely [2-4]. The advantage of this method is similar size and uniformity of nanotubes. However, a difficulty of template removal before using is its disadvantage [5]. On the other hand, soft template has been considered as one of the most promising routes in terms of template-free because of its simplicity, low cost and large-scale production. However, there still exists a problem that the product is usually non-uniform. The different morphologies coexisted in the products such as nanotubes, nanorods, nanoparticles and nanoflakes [6]. It is also noted that different dopants including organic acids and inorganic acids as well as chemical nature of the oxidants, concentration of the reactants (especially of aniline and oxidant) and their molar proportions, presence of additives (i.e. surfactants) affect morphology, formation mechanism and physical properties of PANI [7]. Low concentrations of acids with respect to aniline and the use of organic acids have usually been needed to obtain PANI nanotubes [8].

Recently, the effect of dopant on the morphology of PANI has been studied. Konyushenko et al. [9] have discovered that the morphology of the PANI nanostructures could be affected by varieties of acid in aqueous solution. They reported that polymerization of aniline monomer in a strong acid (sulfuric acid) led to the granular morphology while polymerization in a weak acid (acetic acid) led to the nanotubes. Moreover, Amarnath et al. [10] have discovered that the morphology of the nanostructures could be easily controlled by the concentration of dopant and aniline. Zhang et al. [11-13] reported that PANI nanotubes aggregated to form dendrites when using dopant contained carboxylic acid and hydroxyl group and the diameter increases on increasing the number of -CH_2- groups in the dicarboxylic acids. Then Yin and Yang [14] synthesized the high-performance one-dimensional PANI nanostructures using dodecylbenzene sulfonic acid (DBSA). They reported that PANI nanotubes had a very uniform structure. Huang et al. [6] reported that the synergetic effect of methanol and acetic acid in appropriate proportion can make the PANI nanotubes longer and more uniform.

Nickel is a heavy, silvery-white metal which used in industrial purposes. Nickel can be released into the atmosphere from several industrial processes, including oil and coal burning power plants, trash incinerators, and the metallurgy industry. Thus, the exposure to nickel may take place by air, food samples and drinking water, though mainly by skin contact with contaminated soils and alloys containing nickel. In addition, chronic exposure to high nickel concentrations can cause cancer. Another common disease caused by skin disorder is known as nickel-eczema. The most common reaction is a skin rash at the site of contact. However, in some sensitive people, dermatitis may occur at a site away from the site of contact [15, 16]. On the other hand, drinking water contaminated with nickel can cause nausea, vomit, colic and diarrhea symptom. It also causes nasal cavity cancer and lung cancer. In Thailand, the maximum limit value of nickel contamination is 1 mg/L for industrial wastewater and 0.2 mg/L for drinking water [17].

Conventional technologies for treatment of nickel in wastewater include precipitation, coagulation, reduction, membrane separation, ion exchange, and adsorption. Among these technologies, adsorption has been widely studied because it is easy to operate, cost-effective and unaffected by conventional biological treatments. Many adsorbents have been studied for nickel removal from aqueous solutions, including activated carbons [18, 19], silicates [20-22], polymers [23, 24] and biomass such as bacteria [25] and chitosan [26, 27]. Traditionally, activated carbon has been used as the commonly adsorbent for water treatment but the disadvantage is the difficulties in the reuse process and non-specific. Polymers are an alternative material for removal of specific pollutants from wastewater because it has wide variation in functionality and ease of regeneration. The advantages of polymer are inexpensive, lightweight, easy synthesis and can control the morphology in the synthesis process to obtain a high porosity and surface area. Effective materials for nickel removal generally contain functional groups that have strong interaction with nickel such as sulfur, nitrogen and oxygen [28, 29]. Recently, many research have been reported the use of polymer for Ni(II) removal such as poly (acrylic acid) [30], methacrylic acid/acylamide monomer mixture grafted poly (ethylene terephthalate) [31], poly-ethyleneglycolmethacrylate-*co*-vinylimidazole (PEGMA-*co*-VI) [23] and thiourea-formaldehyde as chelating resin [15]. The advantage of high adsorption capacity, good reusability and high chemical stability were reported.

Recently, Li's group [32, 33] has developed the PANI derivatives adsorbents for removal of metal ions (Hg^{2+}, Pb^{2+}, Ag^{+}). These adsorbents have stronger adsorb ability, faster adsorption rate and lower cost than traditional adsorbents [29]. Since PANI carries large amounts of amine and imine functional groups, this polymer is expected to have interactions with some metal ions having strong affinity to nitrogen. One-dimensional nanostructures such as wires, tubes, and fibers have attracted much attention because they represent the smallest dimensional structures that can be used for efficient charge transport and highly surface area [2, 34-36]. As a result, these materials are expected to be interested in the development of nanoscale application. In the recent research, nanocomposite materials have been used to increase the surface area for adsorption such as PANI coated on rice husk ash [37] and PANI/humic acid [33, 38].

In this research, the synthesis of self-assembled PANI nanotubes doped with different functional groups of organic acids including carboxylic acids (acetic acid and benzoic acid), dicarboxylic acids (malonic acid, lactic acid, malic acid, tartaric acid and citric acid) and sulfonic acids (methanesulfonic acid, *para*-toluenesulfonic acid; *p*-TSA and dodecylbenzene sulfonic acid; DBSA) were studied. Moreover, the synthesis of PANI nanotubes in the presence of methanol was performed. The formation mechanism of one-dimensional PANI nanostructures was discussed based on the relationship between the initial states of soft template and morphologies of the resulting PANI. Moreover, the resulting PANI nanotubes were used for removal of nickel.

1.2 Objective of the research

The objective of this work is to prepare self-assembled PANI nanotubes for efficient removal of nickel(II) in water.

1.3 Scope of the research

1.3.1 Preparation of self-assembled PANI nanotubes with different organic acid dopants
1.3.2 Characterization of PANI nanotubes by scanning electron microscopy (SEM), *transmission* electron microscopy (TEM), fourier transform infrared spectroscopy (FT-IR) and surface area analyzer
1.3.3 Investigating the efficiency of PANI nanotubes for removal of nickel(II) with flame atomic absorption spectroscopy (FAAS)
1.3.4 Study the influence of several parameters on the removal efficiency such as pH of aqueous solution and contact time

1.4 Benefits of the Research

This research aimed to prepare self-assembled PANI nanotubes as the adsorbent for removal of nickel(II).

CHAPTER II

THEORY

2.1 Polyaniline (PANI)

The polyaniline (PANI) constitute a large class of conducting polymers which are formed by the chemical or electrochemical oxidative polymerization of aniline or its derivatives. Some forms of the polymer can be "doped" either chemically or electrochemically with a concomitant increase in electronic conductivity of 10orders of magnitude to produce powders, films or fibers having conductivities in the metallic conducting regime.

The scientist and technologist interest in the PANI stems from the richness of their chemistry and physical properties. Their chemistry, electrochemistry, electronic, magnetic and optical properties can be fine-tuned by the facile synthesis of a large variety of ring- and *N*-substituted derivatives [40].

2.1.1 Properties of polyaniline

PANI is a phenylene-based polymer having –NH– group on either side of the phenylene ring. The general polymeric structure of PANI is shown in Figure 2.1 containing aniline repeating units to form a backbone of alternating nitrogen atoms and benzene rings. The oxidation and reduction takes place on this –NH– group, and various forms are obtained due to the number of imine and amine segments on the PANI chain. Aniline basically undergoes oxidative polymerization in the presence of a protonic acid. The product formed is a simple 1, 4-couplingof the monomer. Protonation induces an insulator-to-conductor transition, while the number of π-electrons in the chain remains constant (Figure 2.2) [41, 42].

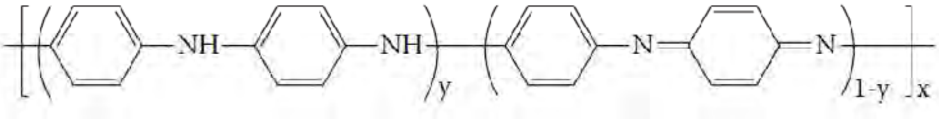

Figure 2.1 The general polymeric structure of PANI [41].

The PANI exists in various oxidation states. Leucoemeraldine base (fully reduced; y=1) is very reactive. It reacts even with minute amount of oxygen and they are environmentally unstable. Pernigraniline base (fully oxidized; y=0) is environmentally stable and further oxidation is not possible with fully imine groups. The ratio of benzenoid to quinoid type is 1:1. Emeraldine base (EB) (partially oxidized; y=0.5) is environmentally stable and does not undergo any change in chemical structure on prolonged storage. Its ratio of benzenoid to quinoid type is 3:1. The fully oxidized and fully reduced state of PANI is not in a conducting state. Therefore the emeraldine base form is the most useful because of high stability at room temperature. The different forms of PANI can be readily converted to one another by simple redox methods. In the principle, the imine nitrogen atoms can be protonated in whole or in part to give the corresponding salts, the degree of protonation of the polymeric base depending on its oxidation state and on the pH of the aqueous acid. Complete protonation of the imine nitrogen atoms in emeraldine base to emeraldine salt (ES) by, e.g. aqueous HCl, results in the formation of a delocalized polysemi-quinone radical cation and is accompanied by an increase in conductivity of ~10^{10} [40, 42].

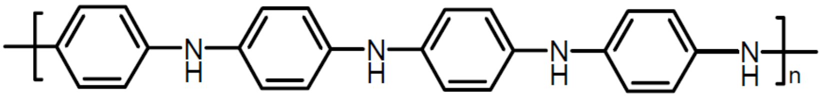

Leucoemeraldine (pale yellow)

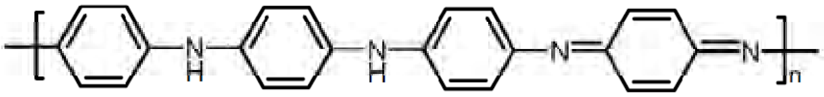

Emeraldine base (blue)

$-\mathrm{H}^+ \rightleftharpoons +\mathrm{H}^+$

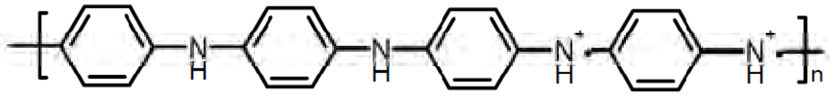

Emeraldine salt (green)

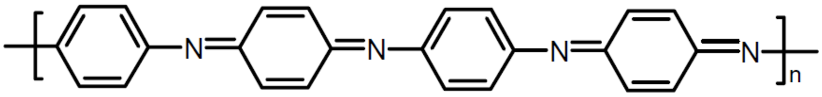

Pernigraniline (violet)

Figure 2.2 Various possible oxidation states of PANI [42].

2.1.2 Synthesis of polyaniline

There are two principal methods for the synthesis of PANI. The first one is the direct oxidation of aniline by chemical oxidants and the second way is through electrooxidation on an inert electrode.

2.1.2.1 Chemical synthesis

Generally, PANI can be synthesized by chemical oxidative polymerization of aniline by several techniques such as aqueous, dispersion, emulsion, inverted emulsion and interfacial polymerization pathway techniques. PANI–ES can be easily obtained as dark green powder by polymerization of aniline in aqueous media using oxidizing agents such as ammonium persulfate, potassium iodate, hydrogen peroxide, potassium dichromate, etc. (Figure 2.3). The main advantage of chemical synthesis is its ease and capability to produce large volumes of PANI in good yield. The reaction is mainly carried out in acidic medium at pH between 0 and 2. The concentration of the monomer employed varies in ranges 0.01 to 1 M. Generally, a stoichiometric equivalent of oxidant is used to avoid degradation of the polymer. Oxidative chemical polymerization is generally carried out at low temperatures (–15 to 5 °C) in order to obtain PANI with high molecular weight. One of the disadvantages of this method stems from the experimental observation that an excess of the oxidant and higher ionic strength of the medium leads to materials that are essentially intractable. In a typical synthesis, aniline (0.1 M) is dissolved in 1 M solution of protonic acid such as HCl, H_2SO_4, $HClO_4$, etc. and is cooled to 0–5 °C. A precooled solution of the oxidant (0.1 M) with or without protonic acid is added drop-wise with continuous stirring for 20–30 minutes. After about 10–15 minutes, the solution gradually develops a green tint. The dark green/blue-green precipitate of emeraldine salt was formed after 6 h, filtered, washed and dried in vacuum for 48 h. Emeraldine base can be obtained by stirring the ES powder in 0.05 M solution of NH_4OH for 10–12 h. The dark blue powder of EB is further washed with 0.05 M NH_4OH and dried under vacuum [42].

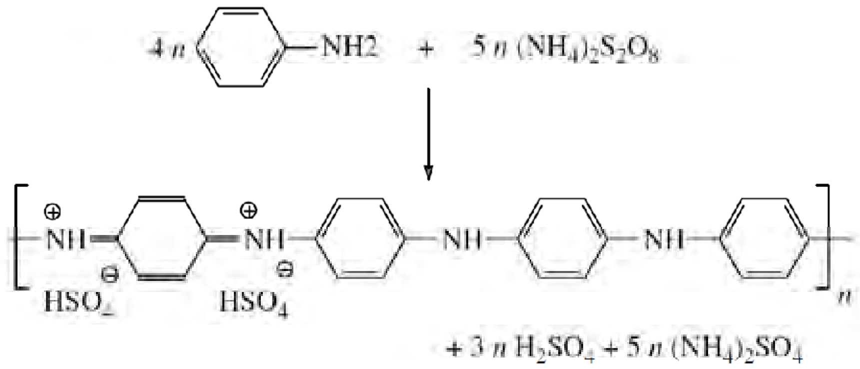

Figure 2.3 Stoichiometry of aniline oxidation with ammonium peroxydisulfate to PANI hydrogen sulfate in an acidic medium [7].

2.1.2.2 Electrochemical synthesis

Electrochemical polymerization became a widely used procedure for quick generation to PANI because none of any surfactant and oxidant in the synthesis process, simpler, quick and perfectly controllable. PANI is easily deposited from aqueous and non-aqueous media, very adherent to many types of substrates and is well-conducting and stable. Electrochemical polymerization uses an initial electrochemical step, generally oxidation via an applied potential to generate the radical ion, which then initiates the polymerization. The method can be used 3 electrode or 2 electrode (working, counter) [43]. It used galvanostatic method which a constant current is applied, including potentiostatic method with a constant potential and potentiodynamic method which current and potential are varied with time. A three-electrode system is the best choice to realize synthesis. The components of system are a working electrode which the polymer is deposited, a counter electrode also named auxiliary electrode (platinum grid) and a reference electrode (in most cases, a saturated calomel electrode (SCE)). Working electrodes produced from various materials have been successfully utilized in depositing conducting polymers, such as gold, platinum, and stainless steel [44]. Deposition of PANI have been achieve onto conducting glass (glass covered by indium-doped tin oxide (ITO) electrode), stainless steel, graphite, Fe, Cu, Au, etc [45]. Electrochemical polymerization exhibits several advantages such as produces thin films with a thickness of few micrometers on an electrode surface, while a chemical oxidation yields a fine-grained material and can be modified in several ways to obtain tailored materials with special functions: (i) derivatization of the monomer by introducing aliphatic chains with functional groups; (ii) variation of the counterion, incorporated for charge compensation during the polymerization process; (iii) inclusion of neutral molecules with special chemical functions and (iv) formation of compounds with noble metal nanoparticles as catalyst for electrochemical oxidation and reduction processes [46].

2.1.3 Polyaniline doping

Until the discovery of the novel protonic acid doping of PANI during which the number of electrons associated with the polymer chain remains unchanged, the doping of all conducting polymers had previously been accomplished by the partial removal (oxidation) or addition (reduction) of electrons from or to the π-system of the polymer backbone (Figure 2.4). The formal rearrangement of electrons in the formula of emeraldine is shown in Figure 2.5. It helps to understand why the protonated emeraldine, a PANI "salt", contains a fraction of unpaired electrons, stable cation-radicals. Two electrons, each from electron pairs on imine nitrogens, are injected into the quininediimine ring. They add the "third double bond" to complete the benzenoid ring. Single unpaired electrons left on nitrogens represent cation-radicals in chemical terminology, and polarons in the realm of physics. The polarons redistribute along the PANI chains to produce a polaron lattice that is responsible for the conductivity of PANI [47].

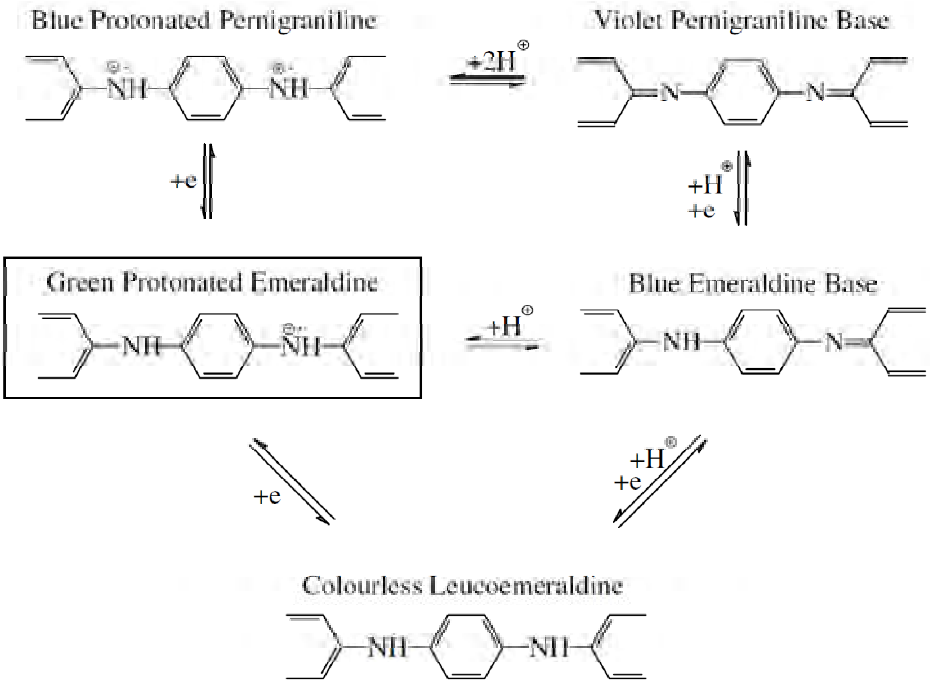

Figure 2.4 Interconversion of different oxidation states of PANI through redox procedure [47].

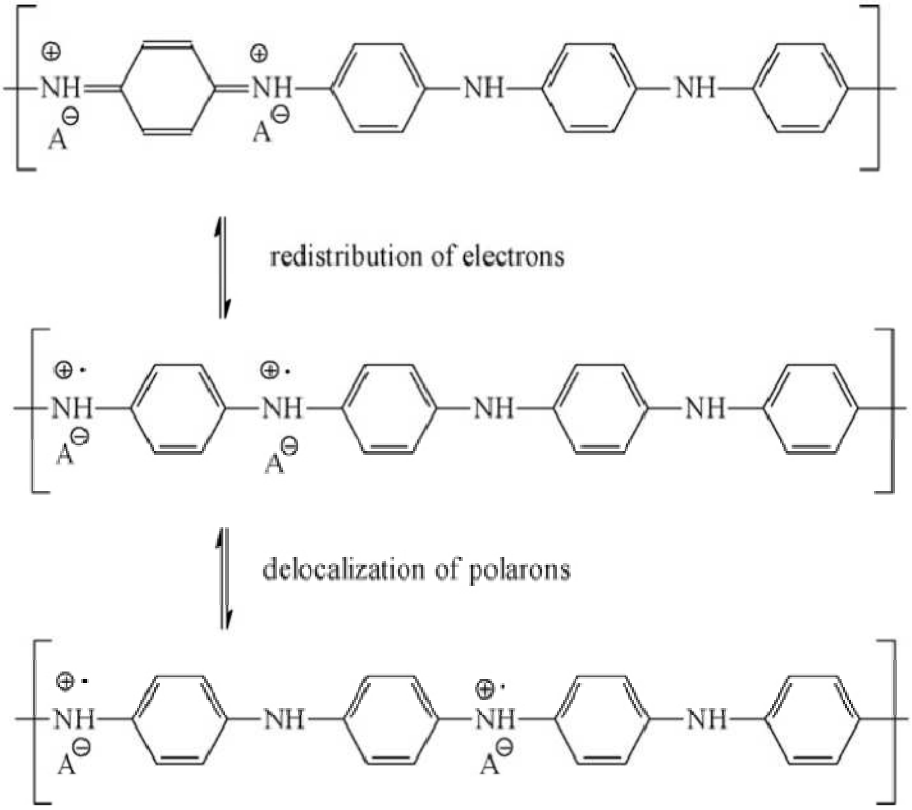

Figure 2.5 Various presentations of protonated emeraldine [7].

The concept of doping is the unique, central, underlying and unifying theme which distinguishes conducting polymers from all other types of polymers. During the doping process, an organic polymer, either an insulator or semiconductor having a small conductivity, typically in the range $10^{-10}$to 10^{-5}S/cm, is converted to conducting regime (~l to ~10^{4} S/cm). The controlled addition of known, usually small (≤10%) and non-stoichiometric quantities of chemical species results in dramatic changes in the electronic, electrical, magnetic, optical and structural properties of the polymer. Doping is reversible to produce the original polymer with little or no degradation of the polymer backbone. Both doping and undoping processes, involving dopant counter ions which stabilize the doped state, may be carried chemically or electrochemically. By adjusting the doping level, a conductivity of the undoped (insulating or semi-conducting) and that of the fully doped (highly conducting) form of the polymer may be easily obtained. Conducting blends of a (doped) conducting polymer with a conventional polymer (insulator), whose conductivity can be adjusted by varying the relative proportions of each polymer, can be made. This permits the optimization of the best properties of each type of polymer [40].

2.2 Polyaniline nanotubes

Polyaniline (PANI) nanotubes are one of the most interesting objects among nanostructures polymer. Nanotubes are one-dimensional objects, differing from nanofibers by the presence of an internal cavity, tens to hundreds nanometers in diameter (Figure 2.6). They have a finite length extending to several micrometers.

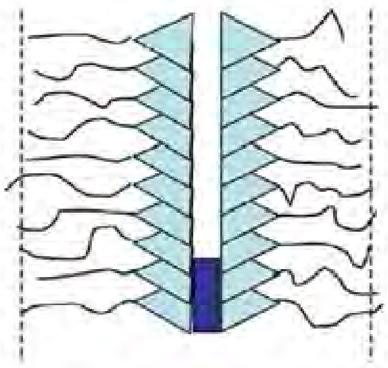

Figure 2.6 Model of nanotube [47].

In contrast to nanofibers, the presence of a template is the necessary condition for the growth of nanotubes. The nanotubes extend to several micrometers in length, they are straight or only slightly curved, and may exceptionallybranch. Several models of nanotubular growth have been proposed in the literature but still not clearly understood. Most of them assume the presence of some template that guides nanotube formation [47].

2.2.1 Hard template synthesis of PANI nanotubes

The hard-template synthesis employs a physical template as a scaffold for the growth of PANI. The hard template scaffold includes colloidal particles and some templates with a nanosized channel, such as anodized alumina oxide and mesoporous silica/carbon templates. For the synthesis using micro/nanoparticles as templates, the target material is precipitated or polymerized on the surface of the template, which results in a core-shell structure. After removal of the template, hollow nanocapsules or nanotubes can be obtained. The most commonly used hard templates include monodispersed inorganic oxide nanoparticles and polymer microspheres. These kinds of templates are advantageous for several reasons: (1) narrow size distribution, (2) ready availability in relatively large amounts, (3) availability in a wide range of sizes from commercial sources, and (4) simplicity of synthesis using well-known formulations. However, the removal of the template often affects the hollow structures. Furthermore, the post-processing for template removal is tedious. The method simplified the process to produce PANI hollow structures in a quantitative way. The only potential drawback of the method is that a reduced emeraldine form of PANI was produced because of the reducibility of template. A template with a nanosized channel can be used to produce conducting polymer nanowires/tubes with a restricted deposition/growth effect. This kind of templating method became a classic method with high controllability to produce nanostructures, and most importantly its arrays. The commonly used and commercially available templates of this sort are anodized alumina oxide membrane, radiation track-etched polycarbonate (PC) membranes, zeolite, and mesoporous carbon [48].

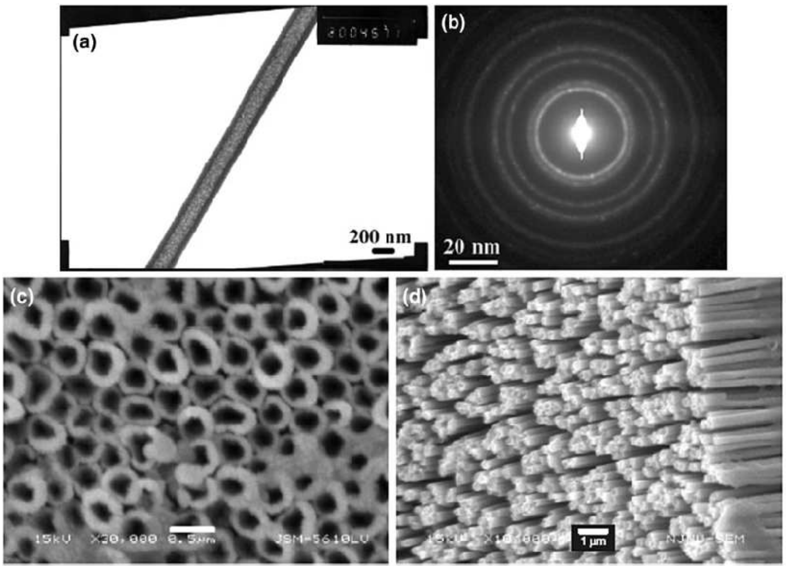

Figure 2.7 a) TEM image and b) selected-area electron diffraction pattern of a Ni nanotube after completely removing the alumina template membrane. c) Top-view and d) side-view SEM images of an ordered-array of Ni nanotubes after partial removal of the alumina template membrane [49].

2.2.2 Soft template synthesis of PANI nanotubes

The soft template synthesis, also named self-assembly, template-free or self-template, relies on molecular self-assembly to form nanostructures. The self-assembly techniques generally favored for their simplicity and high throughput: when nanostructures can be induced to self-assemble, there is no longer a need for external manipulation through templates, lithography or electrospinning (Figure 2.8) [50].

Concerning the formation mechanisms of the nanostructures, it was proposed, but not confirmed, that the surfactants self assembled with or without their aniline salts into nano- or microstructured intermediates due to the hydrophobic property of aniline and the hydrophilic property of the surfactants, which played a template role in forming of the one-dimensional nanostructured PANI. The diameters and lengths of the one-dimensional nanostructured polymer were depended on the factors such as the soft templates, molar ratio of surfactant to aniline, reacting temperature and time and other synthetic conditions [51].

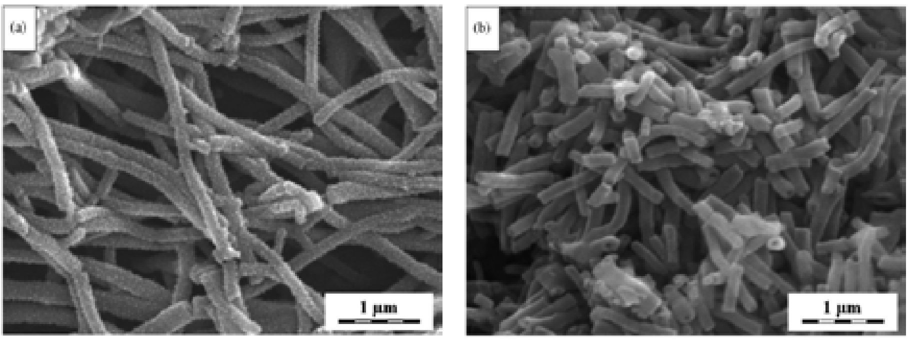

Figure 2.8 SEM image of PANI nanotubes prepared in the presence of (a) succinic and (b) acetic acid [52].

The models of a formation mechanism that have been proposed include phenazine templating [8], micelles as soft template [53] and more recent discoveries such as nanosheet curling [35] and nanoparticle agglomeration [54].

2.2.2.1 Phenazine templating mechanism

The phenazine templating model for PANI nanotubes self-assembly was proposed to the π-π stacking between phenazine-like units, leading to columnar growth. This mechanism has three steps: (1) initial oligomeric crystallite needle, (2) phenazine units absorb onto oligomeric crystallite needle, (3) growth of PANI chains.

The starting point of this mechanism is the presence of aniline oligomers, consisting of 50–60 molecular units that are proposed to form at pH higher than 4 and contain both *ortho*-coupling and *para*-coupling. These early-stage oligomeric products are thought to have low solubility so that they precipitate into “needle-like crystallite offsprings” [8] that serve as templates for the future nucleation of PANI nanotubes (Figure 2.9).The study by Ding et al. [55] on rectangular cross section nanotubes argued intermediates aggregation of aniline oligomers due to their poor solubility, which in turn serve as nucleation sites for growing PANI chains. As the pH is low, some of the oligomers become oxidized, and are proposed to form phenazine units, as shown in Figure 2.10. Then,π-π stacking between the flat molecular structures of phenazine units allows them to absorb on the aforementioned oligomeric needle-like crystals producing columnar aggregates beyond the initial oligomeric templates. Finally, this phenazine units act as starting points for the growth of conventional PANI chains.

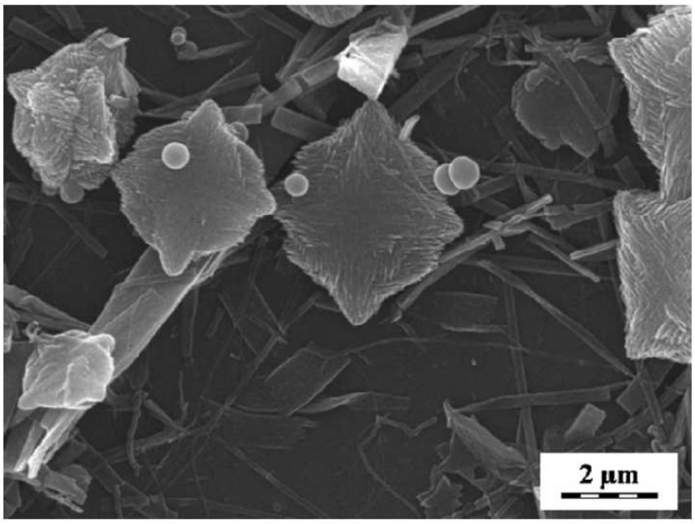

Figure 2.9 The oligomers that precipitate into “needle-like crystallite offsprings” [47].

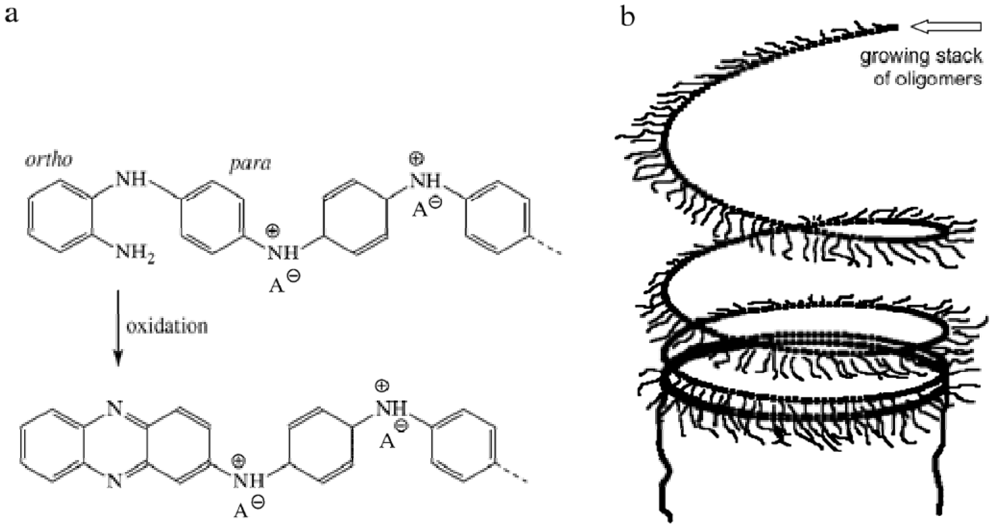

Figure 2.10 The “phenazine theory” formation mechanism (a) First, phenazine units (bottom leftmost corner of figure) form through the oxidation of *ortho*-positioned linked aniline units, positioned as the start of PANI chains. (b) These phenazine units then stack upon each other, stabilized by hydrogen bonding and ionic interactions to form a nanotubular structure [8].

2.2.2.2 Micelles as soft template mechanism

The study that led to the model added β-naphthalene sulfonic acid (β-NSA) to the polymerization reaction [50] in which β-NSA act simultaneously as both a dopant and a surfactant. Since it is a surfactant, β-NSA may then form micelles. The step that then follows is that micelles acting as ‘template-like’ to form a nanotubular or nanofibrous structure by aggregated micelles into bigger spheres and became tubes or fibrils by elongation as shown in Figure 2.11.

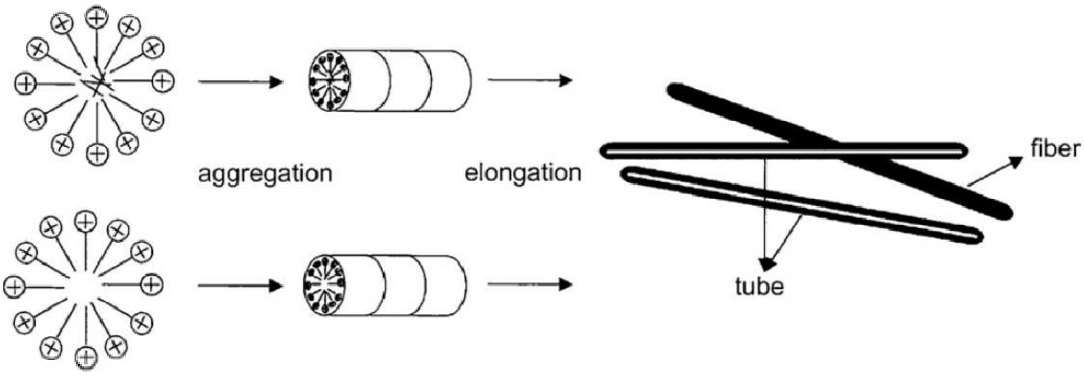

Figure 2.11 Schematic diagram of the “micelles theory” formation mechanism proposed for the self-assembly of PANI nanostructures [50].

Hsieh and et al. [53] also proposed the similar formation mechanism by using dodecylbenzene sulfonic acid (DBSA) and hydrochloric acid (HCl). The following mechanism has been proposed for this theory. The anilinium monomer micelles were derived from the complexation of aniline with DBSA. The inner cores of micelles are hydrophobic long alkyl tails of DBSA and the anilinium ions countered with the aqueous ends of DBSA and well distributed in the outer part of micelles (Figure 2.12). Then, HCl was introduced. The micelles were further expanded by the insertion of the HCl complexed anilinium ions that pointed outward due to their hydrophilic nature of the chloric counter ions (Figure 2.12). Surprisingly, an ordered morphology was found for the micelles solution after treating with HCl. The ordered, supramolecular structures were believed from the ordered alignment of the micelles with the connection of ionic bridges composed of chloric ions as described in Figure 2.13.

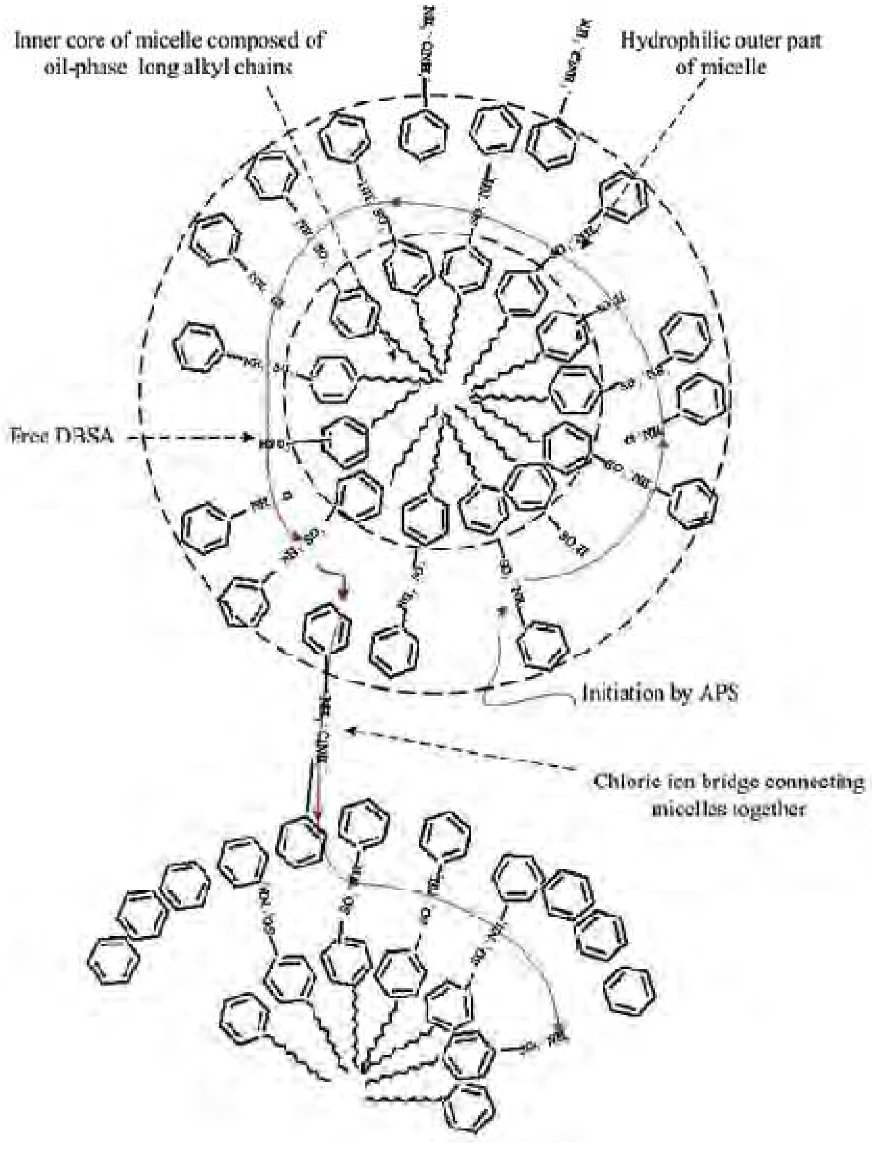

Figure 2.12 Schematic diagram of micelles [53].

With the ignition of the polymerization by hydrophilic APS initiators which are more likely to stay in the hydrophilic outer part of the micelles, the propagation of the polymerization remained in the outer part of the micelles, resulting in the circular conformation of the resultant helical molecules with both complexed and free DBSAs captured inside and the proceeding of the polymerization can extend to neighboring micelles through the chloric ion bridge to create a centipede structure composed of helical molecules which later becomes a nanofibrous or nanotubular structure. The formation of nanotubular PANI from this mechanism could be confirmed by the presence of a centipede-like micrograph of PANI nanotubes (Figure 2.14).

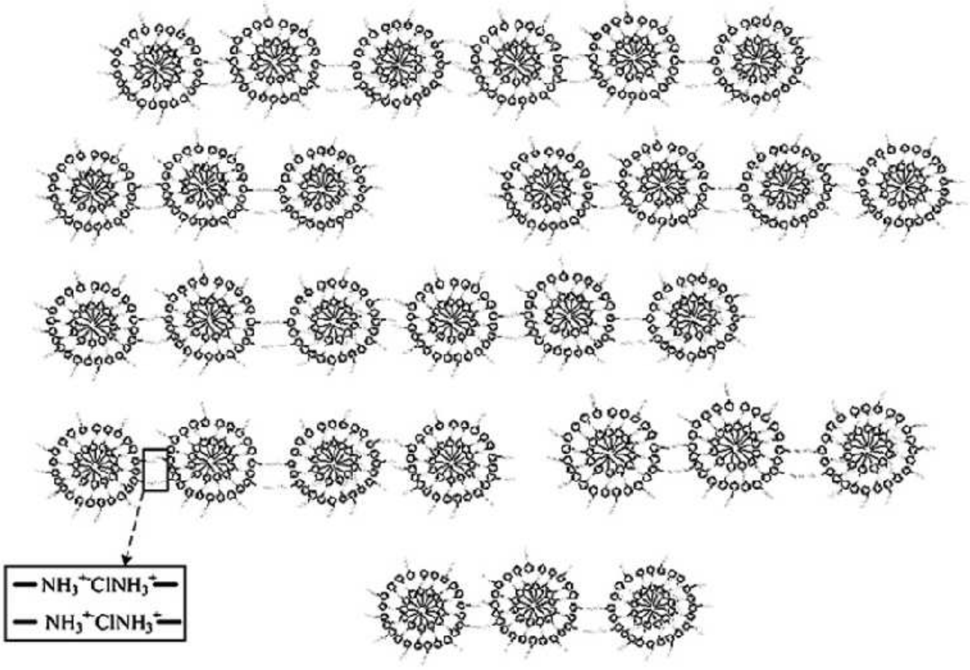

Figure 2.13 LC-like supramolecular structures of associated micelles [53].

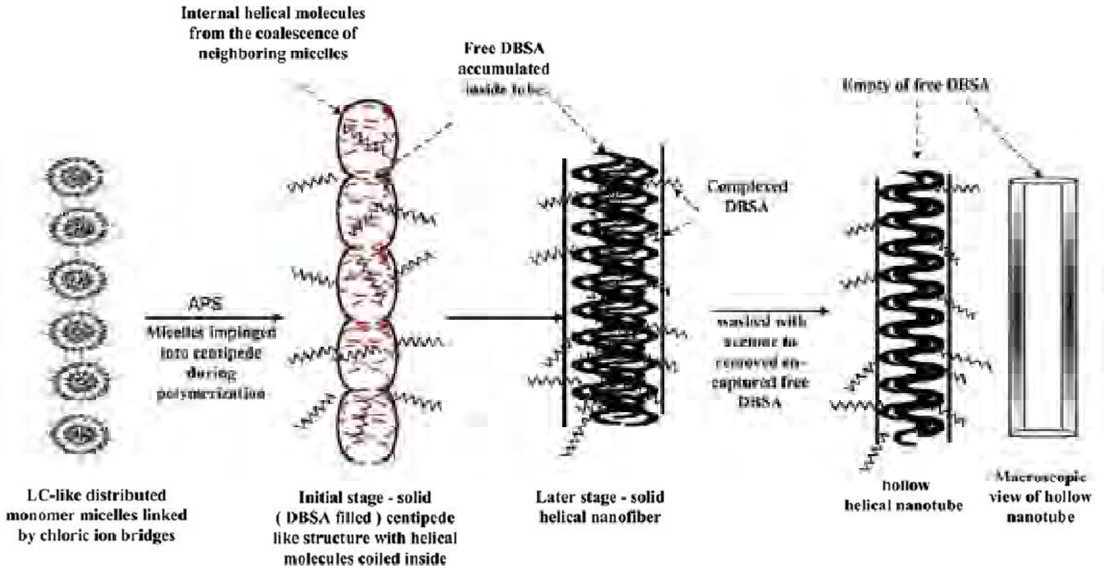

Figure 2.14 Schematic diagram of the formation of PANI nanotubes [53].

2.2.2.3 Nanosheet curling mechanism

Huang and Lin [56] observed this apparent curling during the simplified template-free self-assembly of PANI, that is, during chemical oxidative polymerization without the addition of structurally directing acids. However, they use methanol instead of water, which is the first application of this solvent as a reaction medium during PANI nanotube self-assembly. Their study found that the use of methanol increased yield and uniformity in the resulting nanotubes, which the authors attribute to strong hydrogen bonding that occurs between methanol and the PANI chains. Figure 2.15 illustrates the formation mechanism of PANI nanotubes through several steps in the polymerization. First, the aniline monomers form phenazine-like units with morphology much like tree branches stemming from trunks in the early stages. This is followed by a stage where free aniline monomers diffuse onto the preformed PANI oligomers. The oligomers continue to grow, and form elongated and thickened objects which have a head of phenazine-like units and a tail of *para*-linked aniline units. The protonation of *para*-coupling PANI occurs subsequently, and may provide the primary driving force to cause the trunk and branch of PANI intermediates to curl into nanotubes. The phenazine units, which have nonlinear structures, can serve as the axis for PANI nanotube curling. The final resulting product comprises PANI nanotubes.

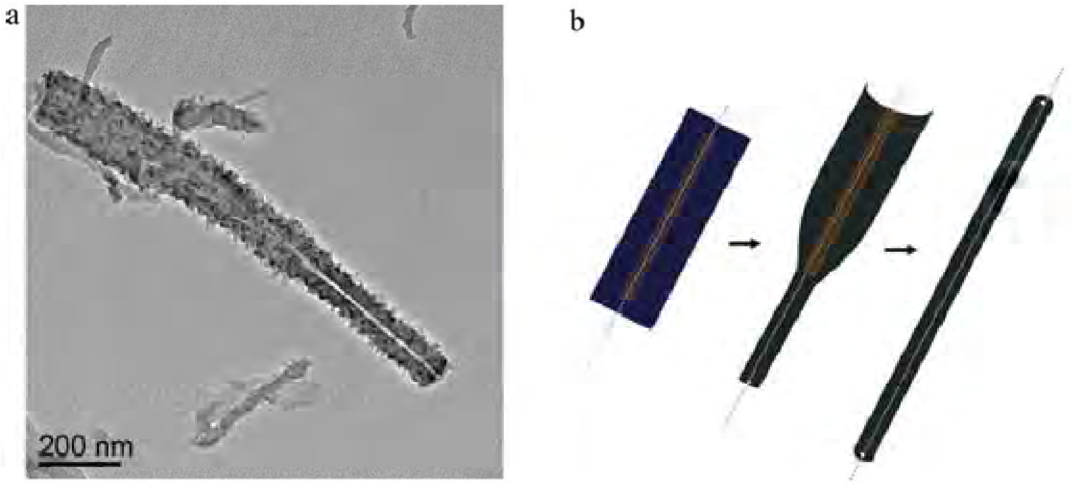

Figure 2.15 (a) TEM image of a semi-curled PANI nanotube, and (b) their accompanying scheme for nanotube formation [50].

2.2.3 Parameters for the formation of PANI nanotubes

2.2.3.1 Dopant

The strength of acidity has a strong influence on the oxidation of aniline and nanotubular structure that shown in Table 2.1 [7]. The courses of aniline oxidation with ammonium peroxydisulfate in aqueous solutions of strong (sulfuric) and in weak (acetic) acids, followed by temperature and acidity changes, are different. In solutions of sulfuric acid, granular PANI (PANI) was produced; in solutions of acetic acid, PANI nanotubes were obtained. The morphology of PANI, granular or tubular, depends on the acidity conditions during the reaction rather than on the chemical nature of the acid [9]. When aniline was oxidized with ammonium peroxydisulfate in aqueous solutions of strong acid, neutral aniline molecule favorably became to anilinium cation radicals that are difficult to oxidize at this stage. Therefore aniline oligomers not formed in this condition. The oligomerization is less favorable in strongly acidic media due to the low concentration of neutral aniline molecules under such conditions. On the other hand, when aniline was oxidized in aqueous solutions of weak acid, neutral aniline molecule were oxidized to oligomers having mixed *ortho-* and *para-* coupled aniline constitutional units. *Ortho*-coupled units may undergo intramolecular cyclization to produce phenazine structures that stack upon each other to form a nanotubular structure (Figure 2.16) [7].

Table 2.1 Properties of PANI prepared in aqueous media of various acidity

	0.1 mol·L^{-1} H_2SO_4	0.4 mol·L^{-1} CH_3COOH	0.2 mol·L^{-1} NH_4OH
starting pH	2.4	4.5	10.4
Terminal pH	1.0	1.1	3.0
Morphology	Granules	Nanotubes	Microspheres
Conductivity of protonated form (S·cm^{-1})	3.7	0.036	$< 10^{-10}$
Conductivity of corresponding base (S·cm^{-1})	1.1 x 10^{-9}	7.9 x 10^{-9}	$< 10^{-10}$
Molecular mass, M_w (g·mol^{-1})	39400	32200	4080
Polydispersity index, M_w/M_n	13.1	19.0	1.3

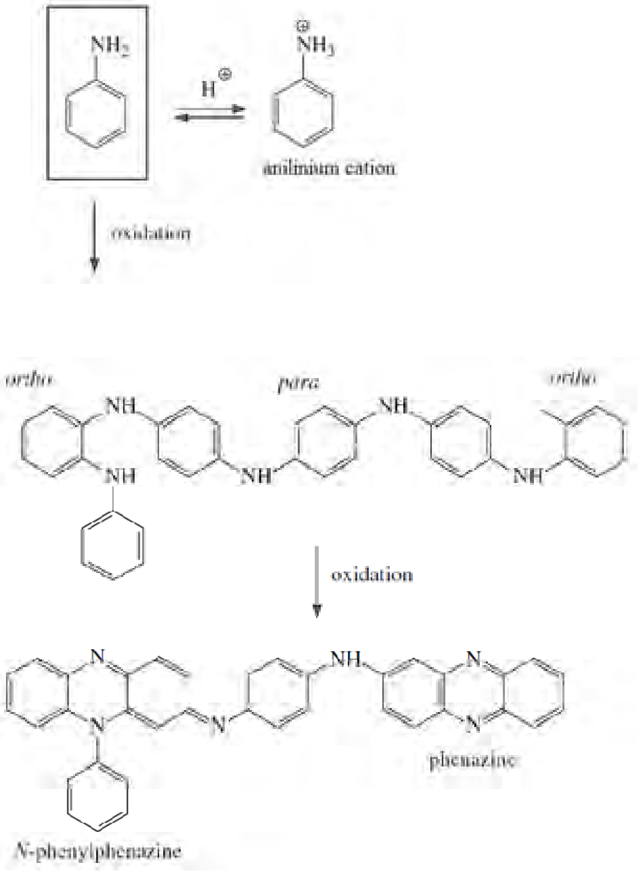

Figure 2.16 Aniline oligomerization [7].

2.2.3.2 pH of reaction solution

Figure 2.17 shown the pH drifts to lower values during the oxidation of aniline and the equilibrium between neutral aniline molecules and anilinium cations shifts in favor of the latter species. As a result, the aniline oligomerization occurs at pH >2. At higher acidity, the conjugated chain structures become protonated and PANI chains grow from initiation centers by adding anilinium cations in *para*-positions. Most of the aniline molecules become protonated at pH <4. Oligomers and polymer chains have terminal primary amine groups with a pK_a value close to that of aniline. There are many ‘internal’ secondary amine units in the chains which are much weaker bases and which become protonated only at pH ~2 and lower.

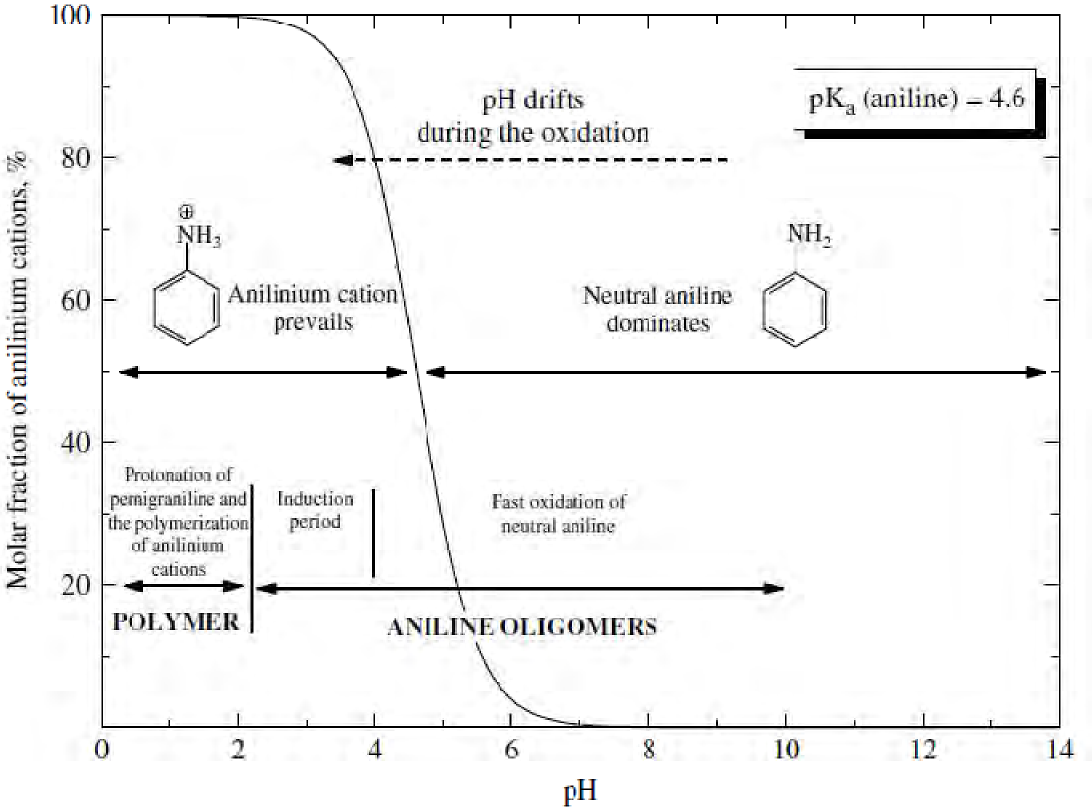

Figure 2.17 The mechanism of oxidation changes as the oxidation proceeds [7].

Under pH >4 of oxidation, all the kinds of amino groups (the aniline monomer, the terminal amino groups in the oligomers and also the secondary amino groups within the oligomer chains) are not protonated. When none of the amino groups are protonated, the monomer and terminal primary amino groups of the oligomers are easily oxidized. The terminal amino group serves as the oxidation centre, which attacks a neutral aniline molecule. The attack is oriented to the *ortho*- and *para*- positions of the benzenoid rings, under the influence of the electron-withdrawing effect of its substituent (the amino group). The ability of an aniline dimer and the oligomers to be oxidized is a few times higher compared with that of the aniline monomer alone due to the better delocalization of the positive charge of the reaction centre on longer molecules. Because of this, the oxidant oxidizes the oligomers with a higher probability than the monomer and the chains elongate (Figure 2.17). In alkaline media, the reaction of aniline addition, i.e. oligomer growth, is faster than the subsequent cyclization reactions. The monomer molecules are converted to oligomers having a mixed coupling structure (Figure 2.18).

In the ranges of pH = 2.5-4, aniline and the primary amino groups in the oligomers become protonated but the secondary amino groups do not. The oxidation is much slower than in alkaline solutions. This is caused by the greatly reduced concentration of oxidizable non-protonated species and increasing fraction of protonated amines, especially anilinium cations (Figure 2.17). The oxidation products are composed of oligomers with *ortho*- and *para*-coupled constitutional aniline units, including phenazine cycles. The formation of cycles represents a large contribution because of the low reaction rates of aniline addition reactions. A large fraction of the oligomers thus contains stable heterocyclic structural units of the phenazine type. Because of that, the oxidation potential of such oligomers increases and approaches the oxidation potential of phenazine cycles (Figure 2.18).

Under pH >2.5 of oxidation, all the primary amino groups and imino groups become protonated. In high acidity condition, the concentration of the easily oxidizable non-protonated aniline molecules is very low and consequently the reaction rate is considerably reduced, so that only short oligomers are produced. Obviously, the formation of oligomers with a sufficiently high degree of conjugation is a prerequisite for the later growth of polymer chains [7-9].

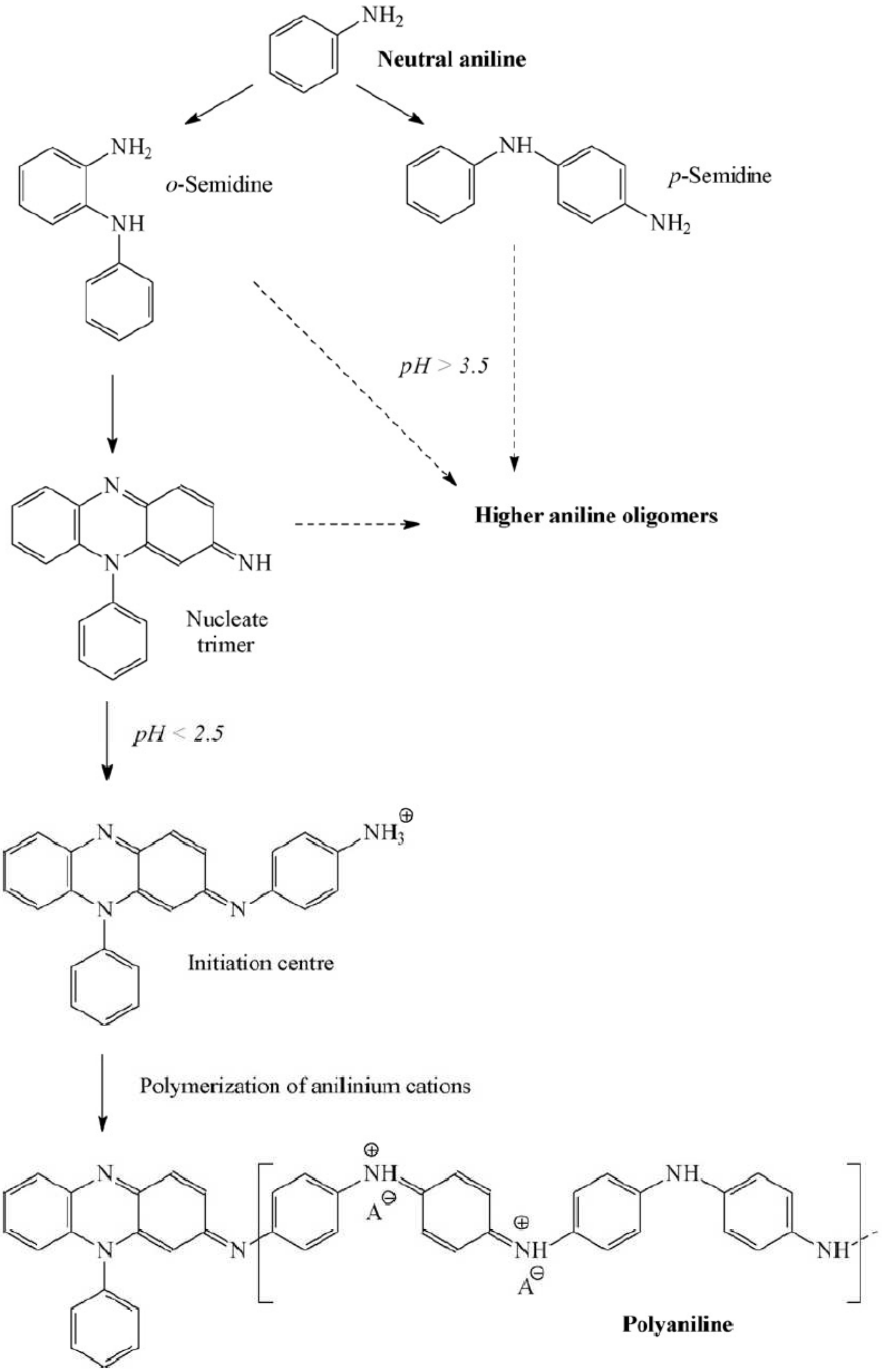

Figure 2.18 The reaction pathways in the oxidation of aniline [47].

2.3 Removal of metal ions using polymers

Polymers have attracted much attention for remove metal ions because they can be readily produced in a wide range of physicochemical properties (size, size distribution, porosity, hydrophobicity, etc.) and they are modifiable by inserting various ligands into the structure in order to make them specific sorbents [57]. For heavy metal ions sorption, the aromatic amine polymers generally posses stronger adsorbability, faster adsorption rate and lower costs than traditional adsorbents such as the activated carbon and chelate resin. Therefore, the aromatic amine polymers would be very useful because metal ions are fairly widespread in our consumer society and probably the most serious toxic metals such as lead, mercury, nickel with cumulative and nondegradative nature [58].

PANI carries large amounts of amine and imine functional groups; therefore PANI is expected to have interactions with some metal ions having strong affinity to nitrogen following by Hard and Soft Acids and Bases (HSAB) theory [28, 59]. The ease with which an acid-base reaction occurs depends on the strength of both the acid and the base. Strong acids and bases are generally more reactive than weak acids and bases. Metal ions have the acceptor atoms and positive charge, so they are acids following by HSAB. On the other hand, polymers that contain various functional groups are bases because they have the donor atoms and negative charge (Table 2.2).

Table 2.2 (1) Characteristics of hard, soft and borderline acids and bases [57]

Type of acid/base	Characteristics	Examples
Hard acids	• Atomic centres of small ionic radii (<90 pm). • High positive charge. • Empty orbitals in their valence shells. • Low electronegativity (0.7-1.6) and low electron affinity. • Likely to be strongly solvated. • High energy LUMO.	H^+, Li^+, Na^+, K^+, Be^{2+}, Mg^{2+}, Ca^{2+}, Sr^{2+}, Sn^{2+}, Al^{3+}, Ga^{3+}, In^{3+}, Cr^{3+}, Co^{3+}, Fe^{3+}, Ir^{3+}, La^{3+}, Si^{4+}, Ti^{4+}, Zr^{4+}, Th^{4+}, VO^{2+} , UO_2^{2+}, $BeMe_2$, BF_3, BCl_3, $B(OR)_3$, $AlMe_3$
Soft acids	• Large radii (>90 pm). • Low or partial positive charge. • Completely filled orbitals in their valence shells. • Intermediate electronegativities (1.9-2.5) • Low energy LUMO's with large magnitude of LUMO coefficients.	Cu^+, Ag^+, Au^+, Hg^+ , Cs^+ , Tl^+ , Hg^{2+} , Pd^{2+}, Cd^{2+} , Pt^{2+} Metal atoms in zero oxidation states
Border line acids		Fe^{2+} , Co^{2+} , Ni^{2+} , Cu^{2+} , Zn^{2+} , Pb^{2+} , $B(CH_3)_3$, SO_2, NO^+

Table 2.2 (2) Characteristics of hard, soft and borderline acids and bases

Type of acid/base	**Characteristics**	**Examples**
Hard bases	- Small radii (around 120pm) & highly solvated. - Electronegative atomic centres (3.0-4.0). - Weakly polarizable. - Difficult to be oxidized. - High energy HOMO.	H_2O, OH^-, F^-, Cl^-, CH_3CO_2-, PO_4^{3-}, SO_4^{2-}, CO_3^{2-}, NO_3^-, ClO_4^-, ROH, RO^-, R_2O, NH_3, RNH_2, N_2H_4
Soft bases	- Large atoms (>170 pm) with intermediate electronegativity (2.5-3.0). - High polarizability. - Easily undergo oxidation. - Low energy HOMO's but large magnitude HOMO coefficients.	RSH, RS^-, R_2S, I^-, CN^-, SCN^-, $S_2O_3^-$, R_3P, R_3As $(RO)_3P$, RNC, CO, C_2H_4, C_6H_6, R^-, H^-
Border line bases		Aniline, pyridine, N_3^-, Br^-, NO_2^-, SO_3^{2-}, N_2

CHAPTER III

EXPERIMENTAL

3.1 Materials

1) Aniline monomer (purity≥99.5%) (Sigma Aldrich, Germany)
2) Dodecylbenzene sulfonic acid (Sigma Aldrich, Germany)
3) Methanesulfonic acid (purity≥99.5%) (Sigma Aldrich, Germany)
4) Tartaric acid (purity≥99.7%) (Sigma Aldrich, Germany)
5) Acetic acid (Merck, Germany)
6) Benzoic acid (Merck, Germany)
7) *p*-Toluenesulfonic acid (Merck, Germany)
8) Malonic acid (Merck, Germany)
9) Lactic acid (Merck, Germany)
10) Malic acid (Merck, Germany)
11) Citric acid (Merck, Germany)
12) Hydrochloric acid (Merck, Germany)
13) Methanol (Sigma Aldrich, Germany)
14) Ammonium peroxydisulfate (Riedel-de Haën, Germany)
15) Nickel(II) sulfate

3.2 Methodology

3.2.1 Preparation of polyaniline nanotube

3.2.1.1 Synthesis through phenazine templating

The self-assembled PANI nanotubes were synthesized based on Huang method [6]. The PANI nanotubes doped with the acetic acid, benzoic acid, malonic acid, lactic acid, malic acid, tartaric acid, citric acid, methanesulfonic acid and *p*-toluenesulfonic acid were prepared by dissolving 0.91 mL of aniline monomer in 50 mL of dopant solution and 2.86 g of ammonium peroxydisulfate (APS) was similarly dissolved in another 50 mL of dopant solution at room temperature. Both aniline monomer and APS solutions were cooled at 0-5°C. After 30 min, rapidly mixed aniline monomer and APS solutions in a beaker and stirred vigorously for 30 s. The mixture was left still to react for 10 h at 0-5°C. The product was filtered and washed with deionized water and finally dried in air for 24 h to obtain the PANI.

The different molar ratios of dopant to aniline (0.01-1) and the addition of methanol (0.01-1 M) in dopant solution were prepared.

3.2.1.2 Synthesis through micelles as soft template

The self-assembled PANI nanotubes were synthesized based on Yin and Yang method [14]. The PANI nanotubes doped with dodecylbenzene sulfonic acid (DBSA) were prepared by dispersing 0.46 g of aniline monomer and 0.326 g of DBSA in 80 mL of deionized water to form slightly cloudy solution. Then 10 mL of HCl solution (0.5 M) was added and it turned to a milky mixture gradually. After 30 min, 10 mL of APS aqueous solution (0.5 M) was added to the above mixture and stirred vigorously for 30 s to initiate the polymerization. Then the reaction was allowed to proceed without agitation for 24 h at 0-5°C. Finally, the precipitates were washed with deionized water and acetone respectively until the filtrate became colorless, and dried in air for 48 h.

3.2.2 Characterization of polyaniline nanotubes

3.2.2.1 Fourier-Transform Infrared Spectroscopy (FT-IR)

FT-IR was used to identify the molecular structures of PANI and confirm the formation of PANI nanotubes. Infrared spectra were recorded by Attenuated Total Reflectance (ATR) and KBr technique using a FT-IR spectrometer (Nicolet 6700, U.S.A.) at the wavenumber range of 400-4000 cm^{-1} using the absorbance mode with 32 scans for ATR and 16 scans for KBr and the wavenumber resolution of ±4 cm^{-1}.

3.2.3.2 Scanning Electron Microscopy (SEM)

The morphologies of PANI were determined using JEOL Scanning Electron Microscope (SEM; model JSM-5410 LV, Japan). The outer diameter of PANI nanotubes was reported as the average values with standard deviation (n=30) by Image Tool 3.0 software (Shareware provided by UTHSCSA).

3.2.3.3 Transmission Electron Microscopy (TEM)

The inner diameter of PANI nanotubes was determined using JEOL Transmission Electron Microscope (JEM−2100).The inner diameter of PANI nanotubes was reported as the average values with standard deviation (n=3) by Image Tool 3.0 software (Shareware provided by UTHSCSA).

3.2.3.4 Nitrogen adsorption-desorption analysis

The nitrogen adsorption−desorption isotherms of PANI nanotubes were measured by a surface area analyzer (BEL, Japan, BELSORP Mini). The Brunauer−Emmett−Teller (BET) equations from adsorption−desorption isotherms were calculated for the determination of surface area and monolayer volume.

3.3 Removal of nickel(II)

3.3.1 Measurement

The concentrations of nickel were measured with a Perkin-Elmer (AAnalyst 100) Flame Atomic Absorption Spectrophotometer (FAAS). Referred to the manufacturer's manual, the operating parameters are as follows: wavelength 232.0 nm and air-acetylene flame. The calibration curve derived from a series of five nickel standard working solutions containing from 1 to 5 mg/L of nickel by appropriate dilution of nickel standard solution (1000 mg/L) with deionized water.

The 1000 mg/L of nickel standard solution was prepared by dissolving 0.4479 g of nickel(II) sulfate ($NiSO_4{\cdot}6H_2O$) in 100 mL of deionized water.

3.3.2 Adsorption procedure

Dried 0.1 g of PANI nanotubes were added into 100 mL reagent bottle that contain 30 mL of 10 mg/L nickel(II) solution and adjusted to desired pH (pH=4-8) by acetate buffer. The solution was stirred during the adsorption at room temperature for a designed contact time (3-24 h). After a designed contact time, PANI nanotubes were removed by filtration. The nickel(II) concentration of the filtrates was analyzed by FAAS. The adsorption amount of nickel(II) onto PANI nanotubes were calculated by using the following equation:

$$Q = \frac{V(C_0 - C_1)}{W}$$

Where Q is the adsorption amount of nickel(II) (mg/g), W is the weight of PANI nanotubes (g), V is the volume of nickel(II) solution (L), and C_0 and C_1 are the concentrations (mg/L) of nickel(II) before and after adsorption, respectively.

The adsorption amount of nickel(II) by resulting PANI nanotubes were compared with commercial PANI particles doped with HCl.

CHAPTER IV

RESULTS AND DISCUSSION

In this research, the synthesis of self-assembled PANI nanotubes doped with different organic acid dopants including acetic acid, benzoic acid, malonic acid, lactic acid, malic acid, tartaric acid, citric acid, methanesulfonic acid, *para*-toluene sulfonic acid (*p*-TSA) and dodecylbenzene sulfonic acid (DBSA) were studied. Then, the removal of nickel in water by synthesized PANI nanotubes was evaluated.

4.1 Synthesis of the self-assembled PANI nanotubes

4.1.1 Formation mechanism

The formation of PANI nanotubes through self-assembly is still not clearly understood although a number of models were proposed. Two models of the formation mechanism that have been mostly described and proposed were the phenazine templating and the micelles as soft template. Ten organic acids contained different functional groups (carboxylic and sulfonic groups) and alkyl moieties (short chain alkyl, long chain alkyl and benzyl) were examined as dopants which are acetic acid, benzoic acid, malonic acid, lactic acid, malic acid, tartaric acid, citric acid, methanesulfonic acid, *p*-TSA and DBSA.

When PANI nanotubes were synthesized through the phenazine templating method as in Section 3.2.1.1, only PANI doped with DBSA did not succeed (Figure 4.1 (a)-(j)). Nanoparticles was obtained. Therefore, the procedure by Yin and Yang method [14] which proposed the synthesis of self-assembled PANI nanotubes through the micelles as soft template was modified. PANI nanotubes was finally achieved as shown in Figure 4.1 (k). However, the co-exist of nanorods and nanoparticles were abundantly observed. Therefore, PANI nanotubes synthesized through phenazine templating method were more uniform and succeed than those through micelles as soft template method.

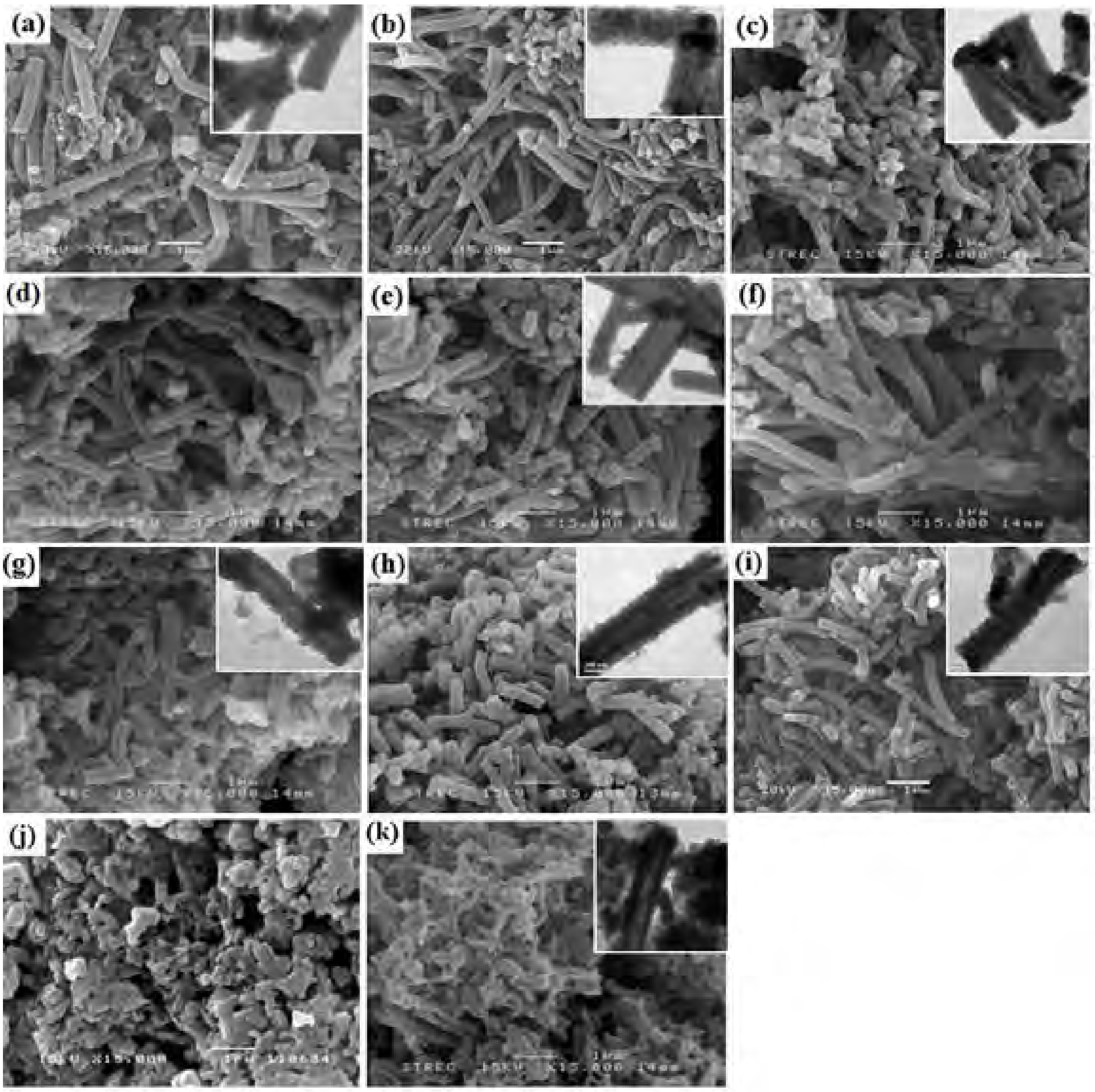

Figure 4.1 SEM images of PANI nanotubes with various dopants and formation mechanism: phenazine templating mechanism, (a) acetic acid (b) benzoic acid (c) malonic acid (d) lactic acid (e) malic acid (f) tartaric acid (g) citric acid (h) methanesulfonic acid (i) *p*-TSA (j) DBSA (Synthetic conditions: [dopant]/[An]=0.2; 0-5 °C; 10 h) and micelle as soft template mechanism (k) DBSA+HCl (Synthetic conditions: [dopant]/[An]=0.2; [HCl]/[An]=1; 0-5 °C; 24 h)

From FTIR spectra, the obtained PANI nanotubes doped with various organic acids were similar as shown in Figure 4.2 (a)-(k) and slightly different from the particles PANI doped with acetic acid (Figure 4.2 (l)). The characteristic peaks of PANI nanotubes and particles in FTIR spectra were summarized in Table 4.1 which are in good agreement with previously reported spectra [6, 8]. The PANI nanotubes showed a slight red shift in the C=C stretching of benzenoid and quinoid rings from 1480 and 1563 cm^{-1} to 1500 and 1587 cm^{-1}, compared with that of PANI particles doped with acetic acid [12].

Table 4.1 The IR characteristic peaks of PANI nanotubes

Functional group	**Wavenumber (cm^{-1})**	
	PANI nanotubes	**PANI particles**
C-H in-plane of quinoid	1587	1560
C-H in-plane of benzenoid	1500	1480
C-C stretching of aromatic	1446	
totally symmetric stretching of the phenazineheterocyclic ring	1414	
C-N stretching of the secondary aromatic amine	1385, 1290	1370, 1292
C-O stretching		1233
N=Q=N (Q: quinoid ring)	1144	
C-H in-plane bending (mode of N=Q=N, $Q=N^{+}H^{-}B$ and $B-N^{+}H^{-}B$)	1123	1110
meta-substituted benzene ring		880
para-disubstitutedbenzoid structure	824	
mono- substituted aromatic rings which located at chain end	695	704

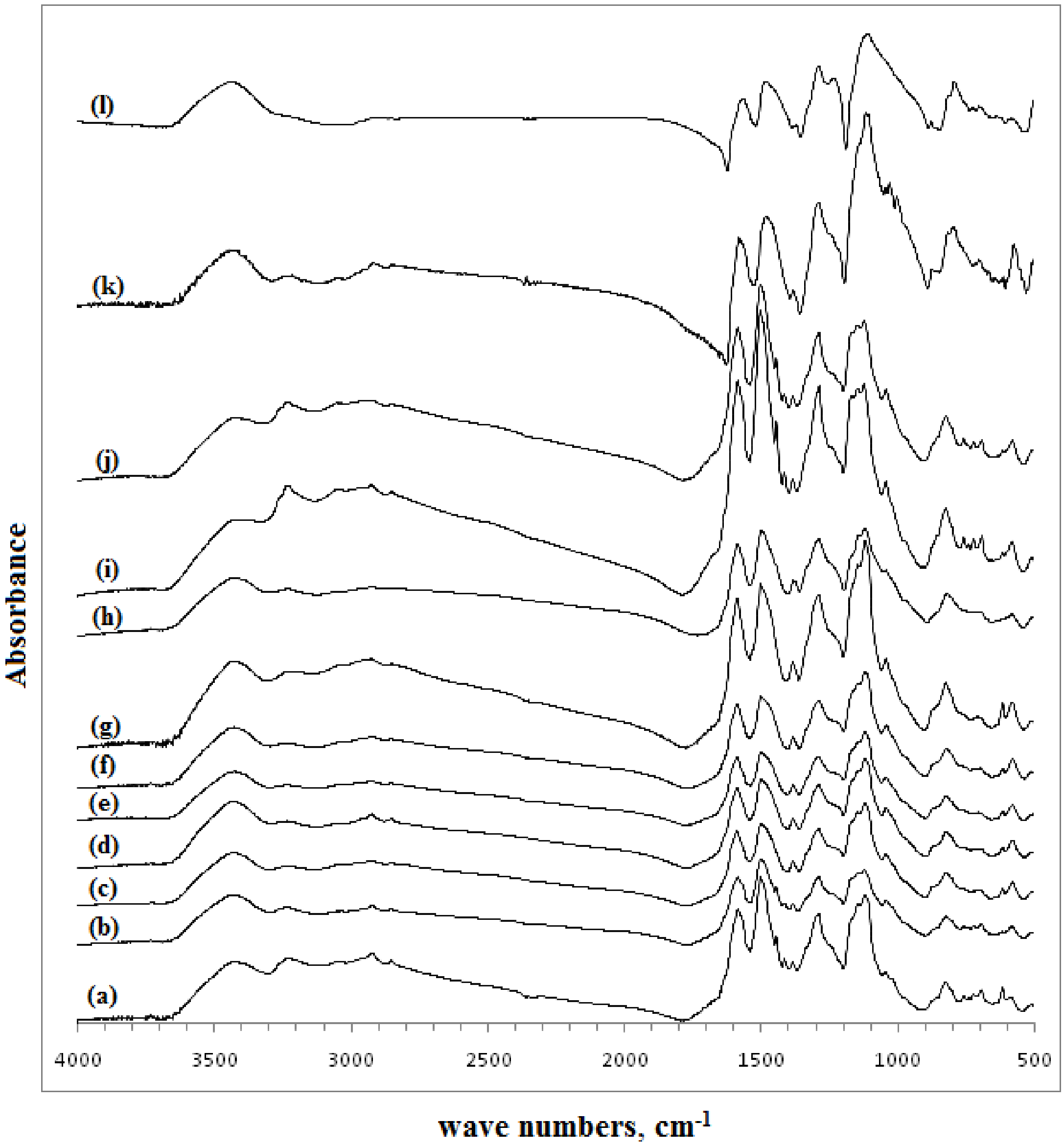

Figure 4.2 FTIR spectra of PANI nanostructures doped with (a) acetic acid, (b) benzoic acid, (c) malonic acid, (d) lactic acid, (e) malic acid, (f) tartaric acid, (g) citric acid (h) methanesulfonic acid, (i) *p*-TSA, (j) *p*-TSA+ methanol (k) DBSA+HCl and (l) PANI particles doped with acetic acid

Moreover, FTIR spectra of PANI intermediates obtained at different reaction times from the synthesis of self-assembled PANI nanotubes through phenazine templating mechanism was observed (Figure 4.3). The intensity of phenazine units peak at 1414 cm^{-1} relative to other PANI characteristic peaks was high during the first hour as phenazine-like units were the initiation center to form PANI nanotubes. After that, the intensity of this peak relative to other PANI characteristic peaks gradually decreased because of the growth of PANI chain [8]. These confirmed the synthesis of self-assembled PANI nanotubes through the phenazine templating mechanism when using the small organic acid dopants which are acetic acid, benzoic acid, malonic acid, lactic acid, malic acid, tartaric acid, citric acid, methanesulfonic acid and *p*-TSA. The self-assembled PANI nanotubes doped with DBSA which is a long hydrophobic hydrocarbon side chains dopant were not noticed this observation and leading to the self assembly through micelles as soft template mechanism instead.

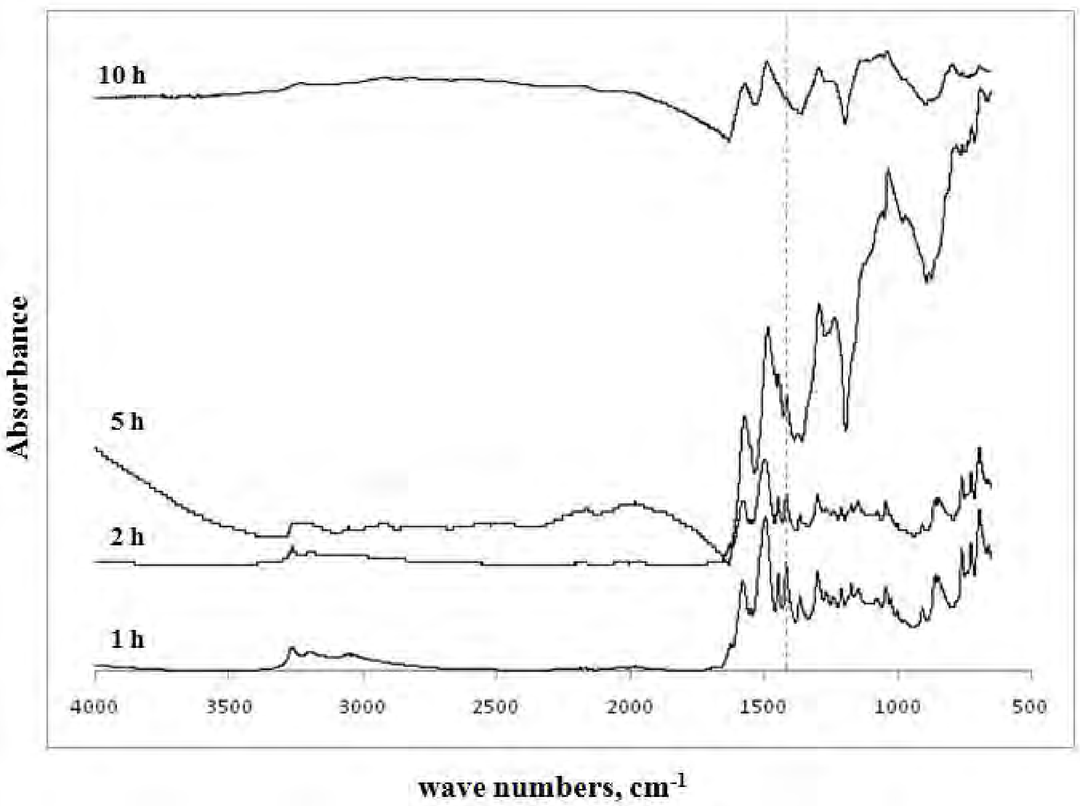

Figure 4.3 FTIR spectra of PANI intermediates obtained at different reaction times. Synthetic conditions: [acetic acid]/ [An] = 0.2.

The average diameter of PANI nanotubes and their surface areas were summarized in Table 4.2. The outer diameters of PANI nanotubes doped with small organic acids (acetic acid, benzoic acid, malonic acid, lactic acid, malic acid, tartaric acid, citric acid, methanesulfonic acid and *p*-TSA) were in the range of 220-330 nm and those doped with long hydrophobic hydrocarbon side chain of organic acid (DBSA) was similar size (260 nm). However, the inner diameter of PANI nanotubes doped with DBSA (120 nm) was larger than those of PANI doped with other small organic acids (8-120 nm). The inner diameter of PANI nanotubes doped with DBSA was agreed with the report of the size of aniline and DBSA micelles which have the averaged size around 91.7 nm [54] since micelles acted as a cores of nanotubular structure of PANI through micelles as soft template mechanism. However, the nanorods that had outer diameter about 110 nm were most obtained when PANI nanotubes doped with DBSA as SEM image shown in Figure 4.1 (k) and related to the outer diameter of nanorods in TEM image. As a result, surface area of PANI doped with DBSA was less than those doped with small organic acids. Furthermore, this might also affect by the aggregation of nanotubes when synthesized PANI through micelles as soft template. Considering the PANI nanotubes doped with small organic acids which synthesized through a phenazine templating mechanism, the surface area of PANI nanotubes doped with malonic acid and malic acid were more than those doped with other dopants since their inner diameters were larger and lot of nanotubes were achieved.

Table 4.2 Diameters and surface area (a_s) of the PANI nanotubes doped with various organic acids.

Dopant	**Molecular formular**	**outer diameter (nm)[a]**	**inner diameter (nm)[b]**	**a_s,BET ($m^2\ g^{-1}$)**
methanesulfonic acid	CH_3-SO_3H	280±20	35±60	17.389
p-TSA	$CH_3(C_6H_4)$-SO_3H	260±30	8±1	16.461
acetic acid	CH_3-COOH	300±30	12±10	17.330
benzoic acid	C_6H_5-COOH	330±30	13±5	16.240
lactic acid	$CH_3CH(OH)$-COOH	240±30		16.895
malonic acid	HOOC-CH_2-COOH	220±20	75±50	26.202
malic acid	HOOC-$CH_2CH(OH)$-COOH	290±40	120±90	22.915
tartaric acid	HOOC-CH(OH)CH(OH)-COOH	350±70		20.068
citric acid	HOOC-$CH_2C(OH)(COOH)CH_2$-COOH	230±30	35±15	16.666
DBSA+HCl	$CH_3(CH_2)_{10}CH_2(C_6H_4)$-$SO_3H$	260±20[c]	120±15	10.362

[a] diameter of PANI nanotubes was averaged from 30 nanotubes from SEM images

[b] inner diameter of PANI nanotubes was averaged from 3 nanotubes from TEM images

[c] outer diameter of PANI nanotubes was averaged from 3 nanotubes from TEM images

4.1.2 Effect of dopants on morphology of PANI nanotubes

The effects of dopants on the morphologies of PANI nanotubes that synthesized through phenazine templating are investigated.

4.1.2.1 Effect of functional group of dopant

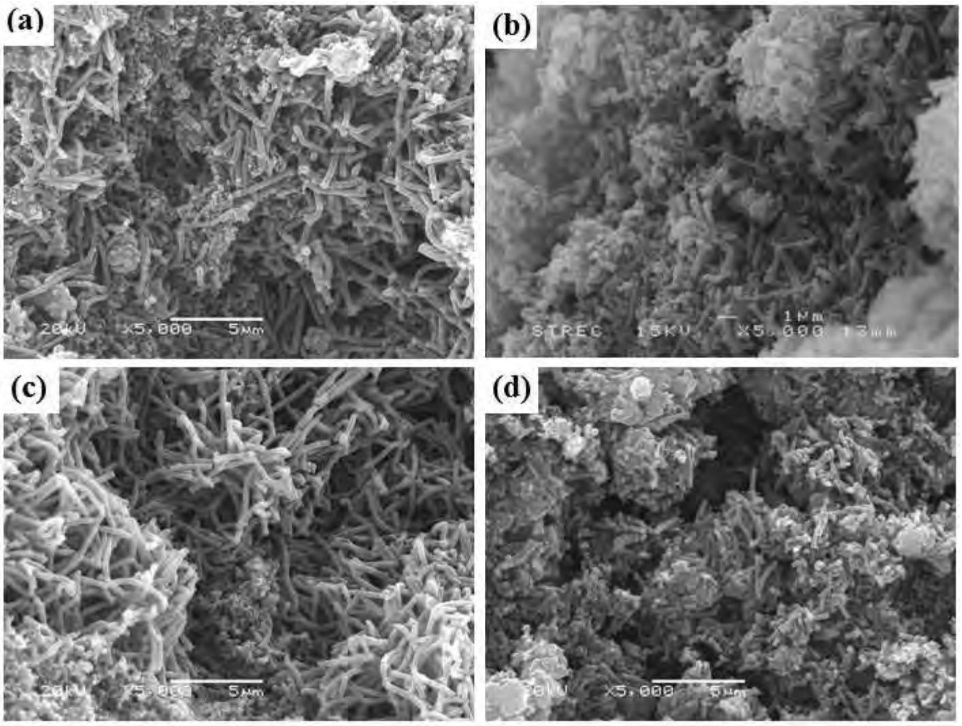

Figure 4.4 SEM images of PANI nanostructures doped with (a) acetic acid, (b) methanesulfonic acid, (c) benzoic acid and (d) *p*-TSA (Synthetic conditions: [dopant]/ [An]=0.2; 0-5 °C; 10 h).

Figure 4.4 (a) and (c) shows that PANI nanotubes doped with organic acid dopants containing carboxylic group were more uniform and less clumping than those doped with organic acid dopants containing sulfonic group (Figure 4.4 (b) and (d)). These might cause by a strong acidity of sulfonic acid, therefore, the pH of the solution at the state of the oxidation and polymerization of PANI was low. As a result, a change of aniline monomer to an anilinium cation was preferable than converting to oligomers that contain phenazine-like unit (see the reaction pathway in Figure 2.19). In Table 4.2, the diameters of nanotubes using carboxylic acid and sulfonic acid dopants were within the same range since the oligomers would precipitate as needle-like crystallite offspring and serve as a template for the growth of nanotubes. PANI nanotubes with an outer diameter of 230-300 nm were achieved when doping PANI with carboxylic acid dopants and 260-280 nm when doping with sulfonic acid dopants. Moreover, inner diameters of PANI nanotubes doped with dicarboxylic acid were larger than those doped with sulfonic acid. When carboxylic acid dopant especially dicarboxylic acid was used, the uniform and long PANI nanotubes were obtained. As a result, surface area of PANI doped with dicarboxylic acid was more than that doped with sulfonic acid.

4.1.2.2 Effect of alkyl and benzyl moieties of dopant

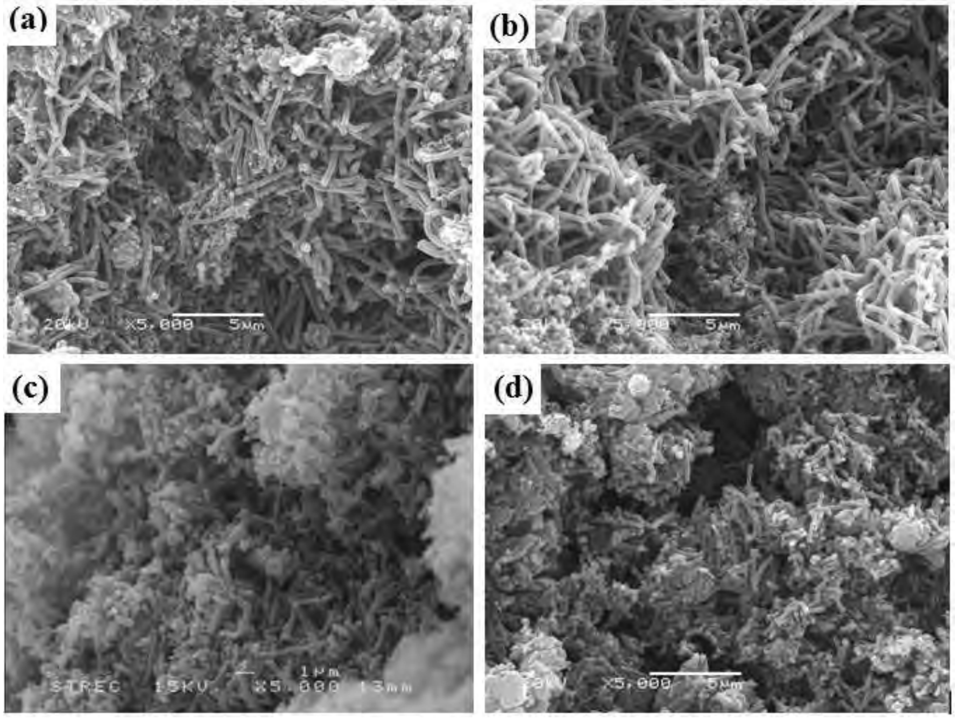

Figure 4.5 SEM images of PANI nanostructures doped with (a) acetic acid, (b) benzoic acid, (c) methanesulfonic acid and (d) *p*-TSA (Synthetic conditions: [dopant]/ [An] =0.2; 0-5 °C; 10 h).

Although, alkyl and benzyl moieties of the dopant were different (acetic acid vs methanesulfonic acid and benzoic acid vs *p*-TSA), the average diameters and surface area of PANI nanotubes were similar (Table 4.1). The morphology and surface area of PANI nanotubes were not affected by different alkyl and benzyl moieties. Since, the acidity of reaction solution plays an important role of PANI nanotubes formation, the small side chain of organic acid might not affect the strength of its acidity comparing to the influence of functional group, and consequently, no effect to the morphology and surface area of PANI nanotubes.

4.1.2.3 Effect of number of carboxylic and hydroxyl groups of dopant

The average outer diameter of the nanotubes increased with the increase of the numbers of carboxylic and hydroxyl groups in dopants, as shown in Table 4.2. As the numbers of carboxylic group in dopants are increased, the bunch of PANI nanotubes was increased. This might cause by the hydrogen bonding between the amine group of the PANI chain and the carboxylic acid groups of the dopant [13]. As a result, PANI nanotubes doped with acetic acid (Figure 4.6 (a)) were more uniform than those doped with malonic acid and citric acid (Figure 4.6 (b) and (f)). Moreover, the additional of hydroxyl group in the dopants yielded the dendrite form of PANI nanotubes [23] as it clearly observed in PANI doped with tartaric acid (Figure 4.7). The hydrogen bonding can form between the amine of the PANI chain and the hydroxyl group and might act as a driving force for aggregation of PANI nanotubes [11]. Therefore, these aggregates might form PANI cores and polymerization of PANI proceeded on this environment can growth as the dendrites [58]. However, the obtained PANI nanotubes were similar in surface area.

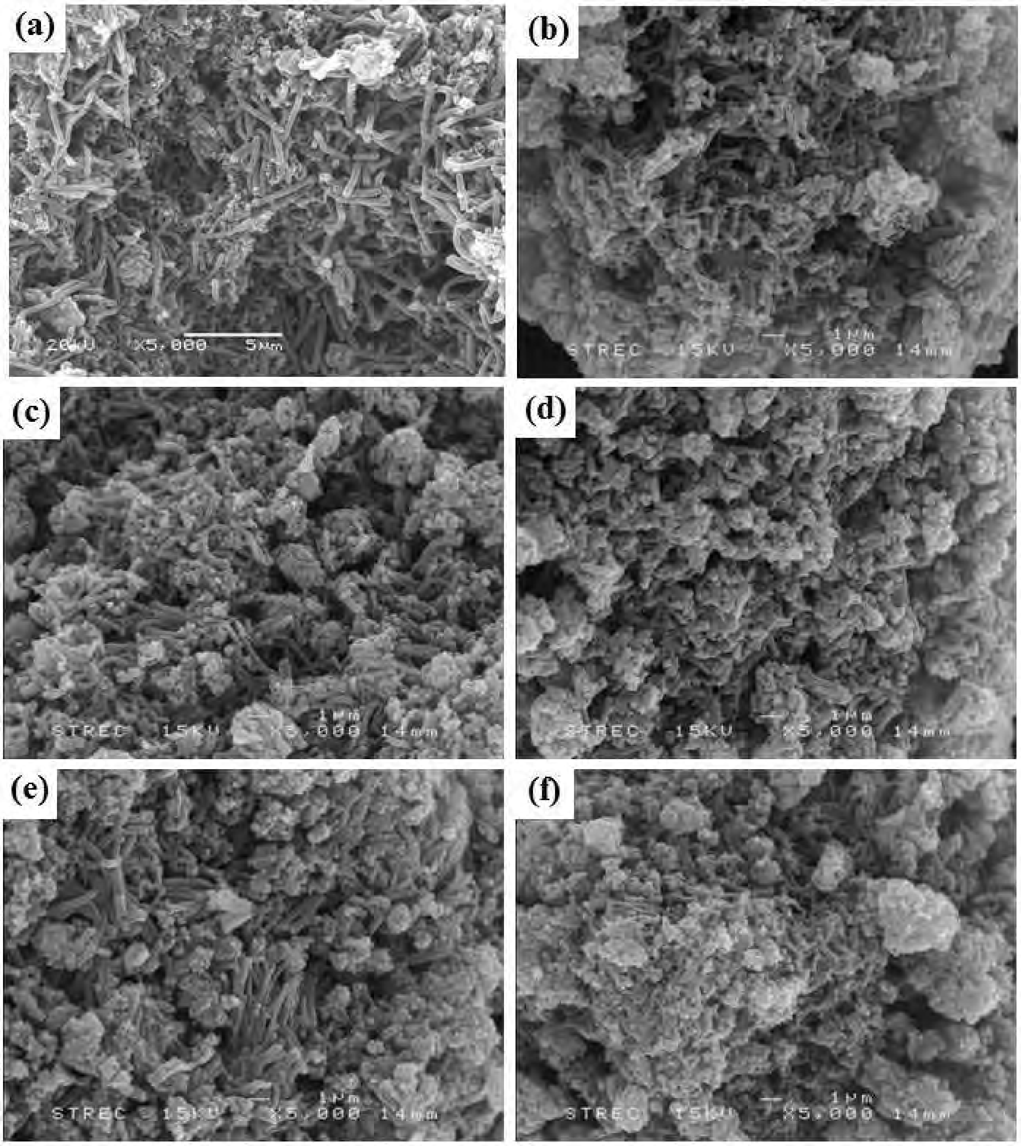

Figure 4.6 SEM images of PANI nanostructures doped with (a) acetic acid, (b) malonic acid, (c) lactic acid, (d) malic acid, (e) tartaric acid and (f) citric acid (Synthetic conditions: [dopant]/ [An] =0.2; 0-5 °C; 10 h).

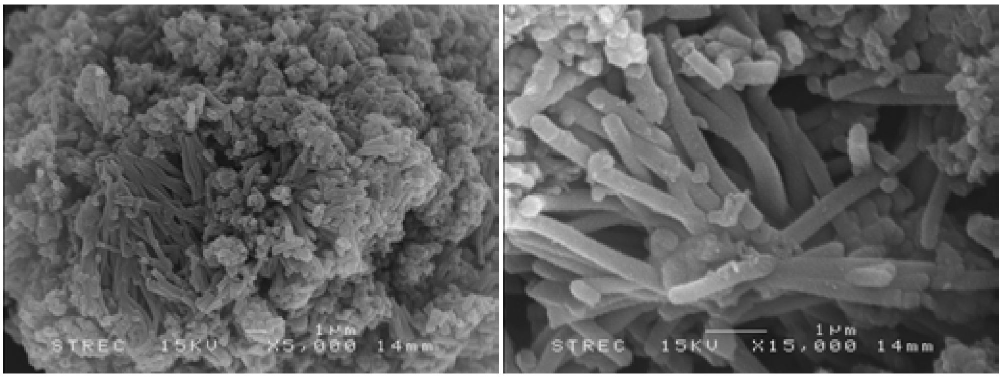

Figure 4.7 SEM images of dendrites formation in PANI doped with tartaric acid (Synthetic conditions: [dopant]/ [An] =0.2; 0-5 °C; 10 h).

4.1.2.4 Effect of methanol

Since the resulting PANI nanotubes that doped with sulfonic acid were aggregated and not uniform, therefore, the PANI synthesis process was improved by adding methanol to push the PANI chain apart [6, 59]. Figure 4.8 shows PANI nanostructures synthesized in the presence of methanol, the nanotubes and nanorods became irregular and lost their uniform morphology which were contrast with Huang's reported [6]. The molar ratio of acetic acid and aniline using in Huang's report were 20 times higher than this research, therefore, a strong intermolecular hydrogen bonding between molecules of PANI and methanol might result in a wrap of PANI chain by methanol molecules. Since the reaction solution in this research contained lower aniline monomer, the hydrogen bonding between PANI chain and methanol would prohibit the self-ordering of PANI chain to form nanotube structures resulting in a formation of aggregated granules instead [11]. The intermolecular hydrogen bonding interaction was interception of PANI chain stacking. Table 4.3 summarized the outer diameter and surface area of PANI nanotubes. The addition of methanol was not affected the outer diameter of PANI nanotubes.

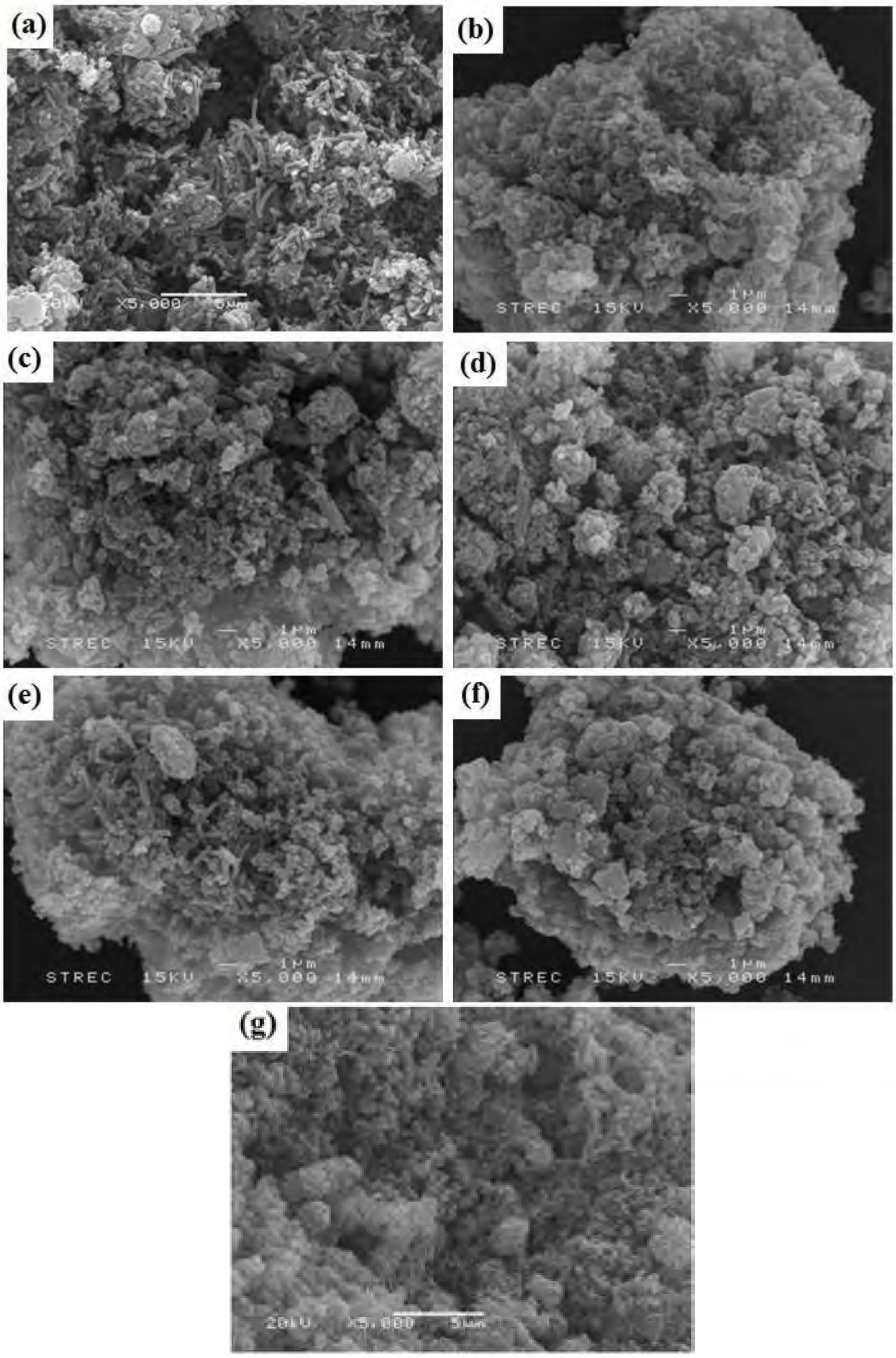

Figure 4.8 SEM images of PANI nanostructures doped with p-TSA in the presence of methanol: (a) no methanol, (b) 0.01 M, (c) 0.05 M, (d) 0.1 M, (e) 0.4 M (f) 0.8 M and (g) 1 M(Synthetic conditions: [dopant]/[An] = 0.2; 0-5 °C; 10 h).

Table 4.3 Effect of methanol on the outer and inner diameters of the PANI nanotubes

Dopant	**Outer diameter**[a]	**a_s, BET**
p-TSA	260±30	16.461
p-TSA+MeOH (0.01 M)	250±20	23.029
p-TSA+MeOH (0.05 M)	230±20	24.070
p-TSA+MeOH (0.1 M)	240±20	30.171
p-TSA+MeOH (0.4 M)	260±30	25.416
p-TSA+MeOH (0.8 M)	300±40	22.453
p-TSA+MeOH (1.0 M)	230±30	15.662
benzoic+MeOH (1.0 M)	310±20	21.390

[a]diameter of PANI nanotubes was averaged from 30 nanotubes

4.1.2.5 Effect of dopant/aniline molar ratio

SEM images of the acetic acid doped PANI prepared at different molar ratios ([acetic acid]/[aniline]) are shown in Figure 4.9. The uniformity of nanotubes was excellent as the molar ratio is 0.2. This molar ratio was produced the optimum starting pH of reaction solution (pH=2.5-4) in which the oxidization of neutral aniline molecules was leading to oligomers having mixed *ortho*- and *para*-coupled aniline constitutional units. *Ortho*-coupled units undergwent intramolecular cyclization to produce phenazine structures that acted as the initiator for the growth of PANI nanotubes. When the reaction occurred at low molar ratio, the solutions had pH greater than 4. Under low acidity conditions, the reaction of aniline addition (i.e. oligomer growth) was faster than the subsequent cyclization reactions. The monomer molecules were converted to oligomers having a mixed coupling structure. On the other hand, when the reaction occurred at high molar ratio, the solutions had pH lower than 2.5. Under conditions of high acidity, the concentration of the easily oxidizable non-protonated aniline molecules was very low, and consequently the reaction rate was considerably reduced. So only short oligomers were produced [7]. However, the sizes of obtained PANI nanotubes at various molar ratios were not different as shown in Table 4.4. Therefore, the different molar ratio of a same dopant did not affect the outer diameter of PANI nanotubes.

Table 4.4 Effect of malar ratio on the outer diameters of the PANI nanotubes

Molar ratio [acetic]/[aniline]	**Outer diameter[a](nm)**
0.01	230±30
0.05	225±25
0.1	280±30
0.2	240±30
0.4	220±30
0.6	240±40
0.8	250±35
1	240±30

[a] diameter of PANI nanotubes was averaged from 30 nanotubes

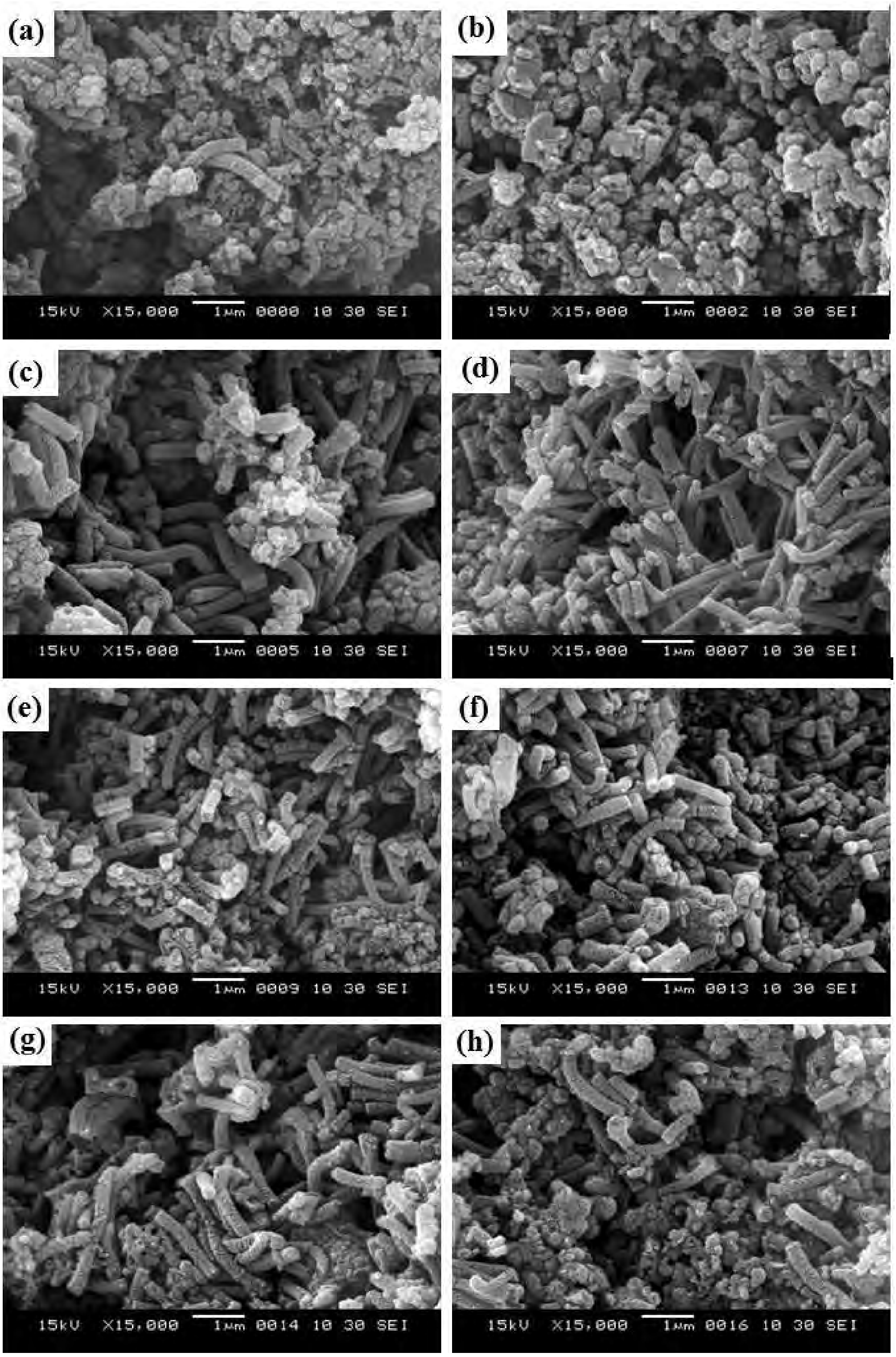

Figure 4.9 SEM images of PANI-acetic acid synthesized using different molar ratios of dopant to aniline, [acetic acid]/[An] : (a) 0.01, (b) 0.05, (c) 0.1, (d) 0.2, (e) 0.4, (f) 0.6, (g) 0.8 and (h) 1.0 (Reaction conditions: [An]/[APS]=1, reaction time =10 h).

4.2 Removal of nickel(II)

PANI carries large amounts of amine and imine functional groups; therefore PANI is expected to have interactions with some metal ions having strong affinity to nitrogen. The main adsorption sites for Ni(II) are the nitrogen atoms in the PANI chains because the nitrogen atom has a lone pair of electrons that can efficiently bind a metal ion through an electron pair sharing to form a complex. A possible adsorption mechanism of Ni(II) ions onto the PANI chains could be a complexation between Ni(II) ions and the nitrogen atoms of amine (-NH-) and doped imine (-$NH^{+\bullet}$-) functional groups [60, 61] similar to the complexation of Hg(II) and PANI proposed by Wang et al. [28].

PANI nanotubes doped with different organic acids including acetic acid, benzoic acid, malonic acid, lactic acid, malic acid, tartaric acid, citric acid, methanesulfonic acid, *p*-TSA and DBSA were examined for the removal of nickel(II) experiments. Figure 4.10 shows the adsorption amount of Ni(II) using PANI nanotubes that doped with various dopants and PANI particles. The adsorption amounts of Ni(II) using all PANI nanotubes accept PANI doped with DBSA (1.85-1.99 mg/g) were almost 4 times greater than that using PANI particles (0.50 mg/g). For PANI doped with DBSA, the adsorption amount was a lot lower than PANI doped with other organic acid dopants (0.76 mg/g). This agreed with the lower surface area of PANI doped with DBSA.

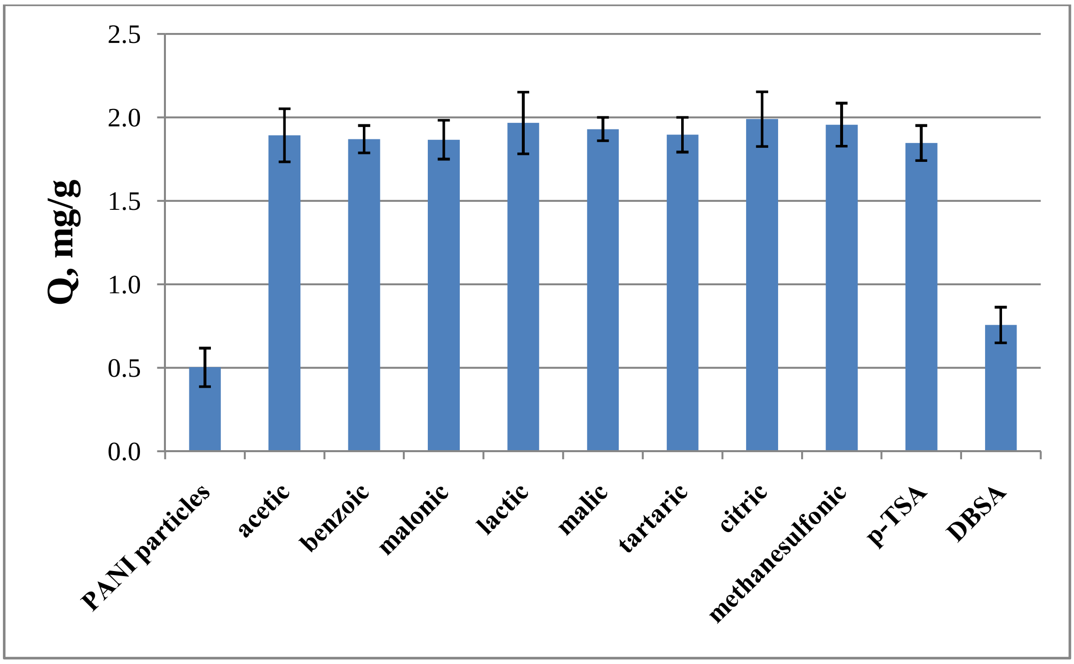

Figure 4.10 Adsorption amount of nickel(II), Q, by PANI nanotubes; adsorption time=18 h, pH=6, C_0=10 ppm.

4.2.1 Effect of contact time

The effect of contact time was studied by selection the resulting PANI that synthesized through different formation mechanism; methanesulfonic acid, *p*-TSA and DBSA. The adsorption amount of Ni(II) increased with the increase of contact time and almost constant when the contact time was over 18 h as shown in Figure 4.11.

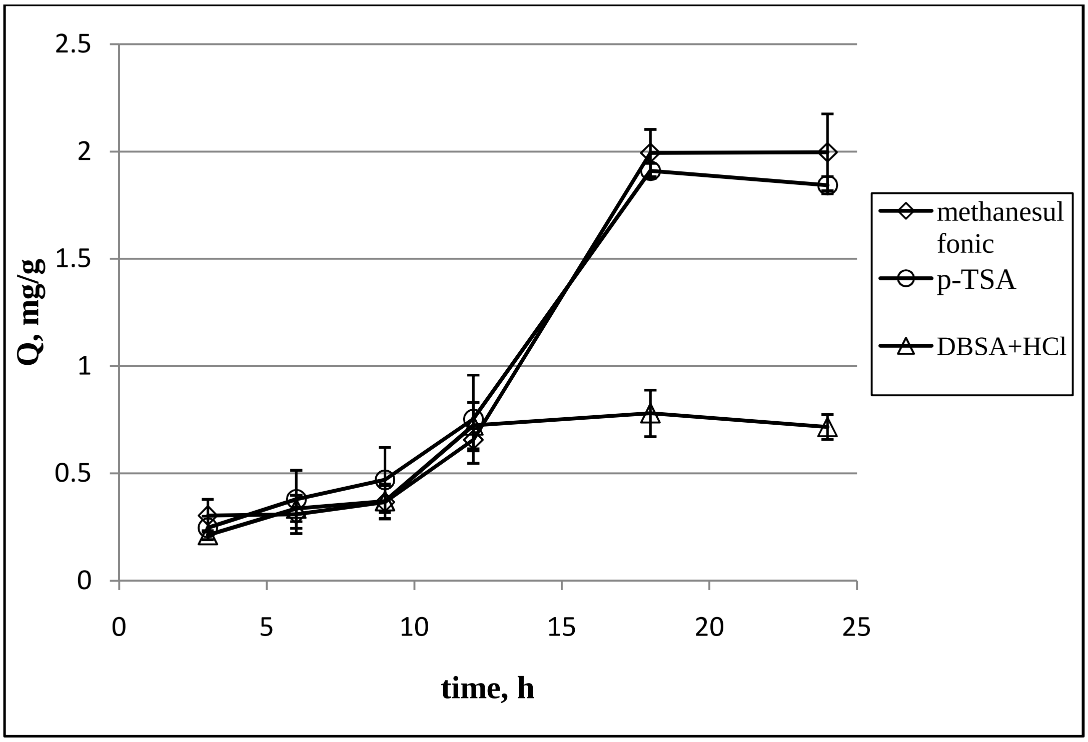

Figure 4.11 Adsorption amount (Q) of Ni(II) onto PANI nanotubes doped with (◇) methanesulfonic acid, (○) *p*-TSA, (△) DBSA+HCl at various contact time; pH=6, C_0=10 ppm.

4.2.2 Effect of pH

The effect of pH of the solution on adsorption of Ni(II) was studied at room temperature by varying the pH from 4-8. The adsorption amount increased when the pH changed from 4 to 6 and then decreased at pH range of 6-8. The maximum adsorption was achieved at pH 6 as shown in Figure 4.12.

Since the protonation and deprotonation behaviors of PANI would be influenced by pH of a solution, the surface structure of the PANI would exist in difference form. At low pH values, protons competitively bound with nitrogen-atoms of the imine in PANI chain (Figure 4.13-1) causing the PANI to carry positive charges. Moreover, the high hydrogen ion concentration at the interface resists positively charge of the Ni(II) ions electrostatically and prevents their approach to the PANI surface [31]. Consequently, the adsorption amountof Ni(II) was low when pH of the solution was acidic. With the increase of solution pH about 5.8, the PANI became less positively charged due to deprotonation and became neutrally charged (Figure 4.13-2). Protons were released from the imine groups (Figure 4.13 (1-2)), leaving more binding sites available for Ni(II) adsorption, resulting in the increase of Ni(II) removal. Further increase pH of solution above 6, the PANI was turned to emeraldine base form, possibly due to competitive specific adsorption of OH^- anions on both imine and amine functional groups (Figure 4.13-3). A slightly decrease of the adsorption capacity was observed.

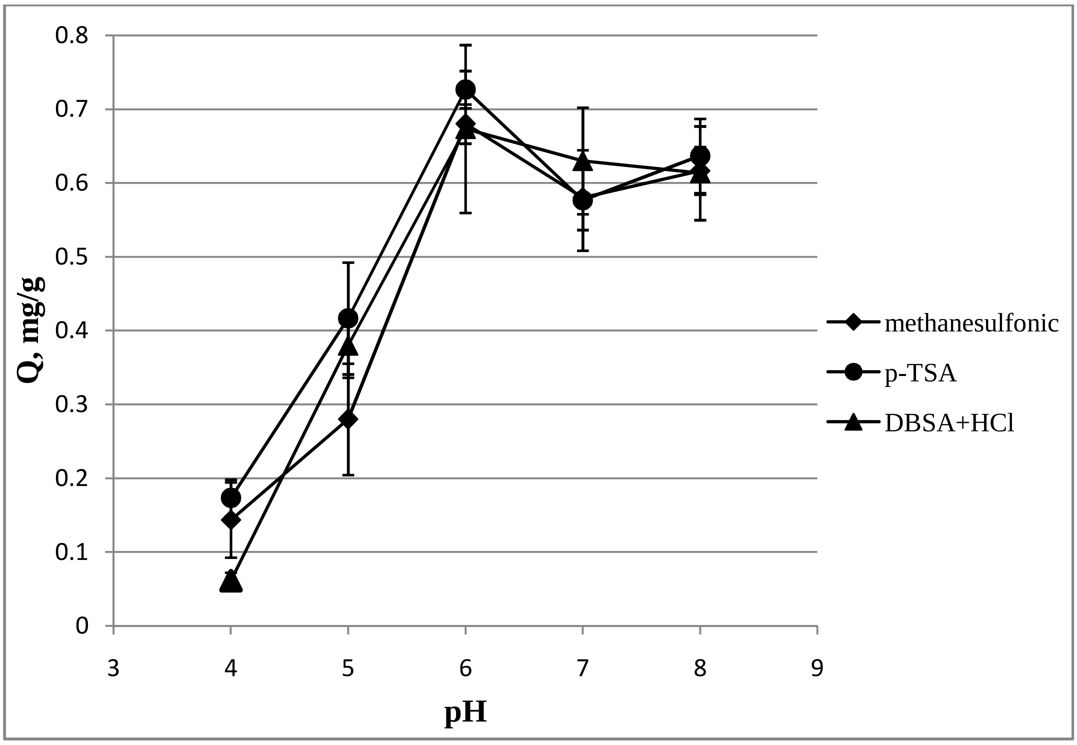

Figure 4.12 Effect of pH on the adsorption amount of Ni(II) on to PANI nanotubes doped with (◇) methanesulfonic acid, (○) *p*-TSA, (△) DBSA+HCl; t=12 h, C_0=10 ppm.

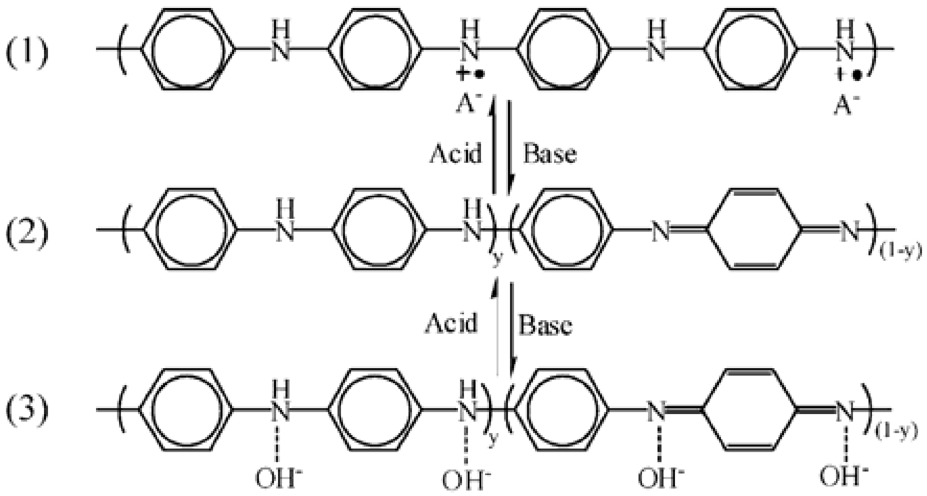

Figure 4.13 Physicochemical properties of PANI in aqueous solutions as a function of solution pH [28].

CHAPTER V

CONCLUSION

5.1 Conclusion

We have successfully prepared the PANI nanotubes through self-assembly method for removal of Ni(II). PANI nanotubes doped with various organic acids were prepared through a self-assembly method. The small organic acid dopants were leading to phenazine templating mechanism of self-assembled PANI nanotubes while the long hydrophobic were leading to micelles as soft template mechanism. The oxidation of some oligomers to form phenazine units for PANI nanotubes through phenazine templating can confirm by the FTIR peak at 1414 cm^{-1}. All the nanostructures formed by doping PANI with different acids were nanotubes but nanorods and nanoparticles also co-exist. The outer diameters of PANI nanotubes doped with small organic acids (acetic acid, benzoic acid, malonic acid, lactic acid, malic acid, tartaric acid, citric acid, methanesulfonic acid and *p*-TSA) were in the range of 220-330 nm and those doped with long hydrophobic hydrocarbon side chain of organic acid (DBSA) was similar size (260 nm). The inner diameter of PANI nanotubes doped with DBSA (120 nm) was larger than those of PANI doped with other small organic acids (8-120 nm). However, the nanorods that had outer diameter about 110 nm were most obtained when PANI nanotubes doped with DBSA. The effects of dopants on the morphologies of PANI that synthesized through phenazine templating are investigated. PANI nanotubes doped with carboxylic acid dopants were more uniform than those doped with sulfonic acid dopants. Since pH of reaction medium was a critical factor in aniline oxidation and production of PANI nanotubes, the acidity of dopants was affected the obtained PANI nanotubes. However, alkyl and benzyl moieties contained in dopants insignificantly affected the morphology of PANI nanotubes. When the carboxylic acid dopants contain hydroxyl group, the PANI nanotubes aggregated to formed dendrites. For the additional of methanol in reaction solution, the nanotubes and nanorods became irregular and lost their uniform morphology. Therefore, it can conclude that the formation yield, size and uniformity of PANI nanotubes were affected by dopants, formation mechanism, reaction media and [dopant]/[aniline] molar ratio.

PANI nanotubes can be used for removal of Ni(II) ions in solution. The adsorption capacity of PANI nanotubes that doped with various dopants was similar. The removal of Ni(II) performance was improved by varied a contact time and pH of the solution. The suitable condition that result the maximum adsorption amount was pH 6 and contact time of 18 h.

REFERENCES

[1] Ren, L. and Zhang, X. F. Preparation and characterization of polyaniline micro/nanotubes with dopant acid mordant dark yellow GG. Synthetic Metals 160 (2010): 783-787.

[2] Tran, H. D., Li, D. and Kaner, R. B. One-Dimensional Conducting Polymer Nanostructures: Bulk Synthesis and Applications. Advanced Materials 21 (2009): 1487-1499.

[3] Garai, A. and Nandi, A. K. Tuning of different polyaniline nanostructures from a coacervate gel/sol template. Synthetic Metals 159 (2009): 757-760.

[4] Martín, J., Hernández-Vélez, M., de Abril, O., Luna, C., Munoz-Martin, A., Vázquez, M. and Mijangos, C. Fabrication and characterization of polymer-based magnetic composite nanotubes and nanorods. European Polymer Journal 48 (2012): 712-719.

[5] Xiong, S., Wang, Q. and Xia, H. Preparation of polyaniline nanotubes array based on anodic aluminum oxide template. Materials Research Bulletin 39 (2004): 1569-1580.

[6] Huang, Z., Liu, E., Shen, H., Xiang, X., Tian, Y., Xiao, C. and Mao, Z. Preparation of polyaniline nanotubes by a template-free self-assembly method. Materials Letters 65 (2011): 2015-2018.

[7] Sapurina, I. and Stejskal, J. The mechanism of the oxidative polymerization of aniline and the formation of supramolecular polyaniline structures. Polymer International 57 (2008): 1295-1325.

[8] Stejskal, J., Sapurina, I., Trchova, M., Konyushenko, E. N. and Holler, P. The genesis of polyaniline nanotubes. Polymer 47 (2006): 8253-8262.

[9] Konyushenko, E. N., Stejskal, J., Šeděnková, I., Trchová, M., Sapurina, I., Cieslar, M. and Prokeš, J. Polyaniline nanotubes: conditions of formation. Polymer International 55 (2006): 31-39.

[10] Amarnath, C. A., Kim, J., Kim, K., Choi, J. and Sohn, D. Nanoflakes to nanorods and nanospheres transition of selenious acid doped polyaniline. Polymer 49 (2008): 432-437.

[11] Zhang, L., Long, Y., Chen, Z. and Wan, M. The effect of hydrogen bonding on self-assembled polyaniline nanostructures. Advanced Functional Materials 14 (2004): 693-698.

[12] Zhang, L. and Wan, M. Chiral polyaniline nanotubes synthesized via a self-assembly process. Thin Solid Films 477 (2005): 24-31.

[13] Zhang, Z., Wan, M. and Wei, Y. Highly crystalline polyaniline nanostructures doped with dicarboxylic acids. Advanced Functional Materials 16 (2006): 1100-1104.

[14] Yin, H. and Yang, J. Synthesis of high-performance one-dimensional polyaniline nanostructures using dodecylbenzene sulfonic acid as soft template. Materials Letters 65 (2011): 850-853.

[15] Ahmad Panahi, H., Mehrdad Sharif, A. A., Bigonah, M. and Moniri, E. Determination and preconcentration of nickel in water with flame atomic absorption spectrometry by thioureaformaldehyde as chelating resin. Arabian Journal for Science and Engineering (AJSE) 35 (2010): 149-162.

[16] Irwin, R. J., Mouwerik, M. V., Stevens, L., Seese, M. D. and Basham, W. Environmental contaminants encyclopedia nickel entry (1997): National park service water resources divisions, water operations branch and assistance from Colorado State University.

[17] Ministry of Natural Resources and Environment of Thailand. Water Quality Standards [Online], 16 April 2013. Source www.pcd.go.th/info_serv/reg_std_ water01.html.

[18] Namasivayam, C. and Kadirvelu, K. Uptake of mercury (II) from wastewater by activated carbon from an unwanted agricultural solid by-product: coirpith. Carbon 37 (1999): 79-84.

[19] Budinova, T., Savova, D., Petrov, N., Razvigorova, M., Minkova, V., Ciliz, N., Apak, E. and Ekinci, E. Mercury Adsorption by Different Modifications of Furfural Adsorbent. Industrial & Engineering Chemistry Research 42 (2003): 2223-2229.

[20] Feng, X., Fryxell, G. E., Wang, L.-Q., Kim, A. Y., Liu, J. and Kemner, K. M. Functionalized Monolayers on Ordered Mesoporous Supports. Science 276 (1997): 923-926.

[21] Mercier, L. and Pinnavaia, T. J. A functionalized porous clay heterostructure for heavy metal ion (Hg^{2+}) trapping. Microporous and Mesoporous Materials 20 (1998): 101-106.

[22] Guerra, D. L., Airoldi, C. and Viana, R. R. RETRACTED: Performance of modified montmorillonite clay in mercury adsorption process and thermo-dynamic studies. Inorganic Chemistry Communications 11 (2008): 20-23.

[23] UgŸuzdogŸan, E., DenkbasŸŸ, E. B. and Kabasakal, O. S. The use of poly-ethyleneglycolmethacrylate-*co*-vinylimidazole (PEGMA-*co*-VI) micro-spheres for the removal of nickel(II) and chromium(VI) ions. Journal of Hazardous Materials 177 (2010): 119-125.

[24] Mansour, M. S., Ossman, M. E. and Farag, H. A. Removal of Cd (II) ion from waste water by adsorption onto polyaniline coated on sawdust. Desalination 272 (2011): 301-305.

[25] Das, S. K., Das, A. R. and Guha, A. K. A Study on the Adsorption Mechanism of Mercury on Aspergillus versicolor Biomass. Environmental Science & Technology 41 (2007): 8281-8287.

[26] Li, N., Bai, R. and Liu, C. Enhanced and Selective Adsorption of Mercury Ions on Chitosan Beads Grafted with Polyacrylamide via Surface-Initiated Atom Transfer Radical Polymerization. Langmuir 21 (2005): 11780-11787.

[27] Vieira, R. S. and Beppu, M. M. Interaction of natural and crosslinked chitosan membranes with Hg(II) ions. Colloids and Surfaces A: Physicochemical and Engineering Aspects 279 (2006): 196-207.

[28] Wang, J., Deng, B., Chen, H., Wang, X. and Zheng, J. Removal of aqueous Hg(II) by polyaniline: sorption characteristics and mechanisms. Environmental Science & Technology 43 (2009): 5223-5228.

[29] Ai, L., Jiang, J. and Zhang, R. Uniform polyaniline microspheres: a novel adsorbent for dye removal from aqueous solution. Synthetic Metals 160 (2010): 762-767.

[30] Morlay, C., Cromer, M. and Vittori, O. The removal of copper (II) and nickel (II) from dilute aqueous solution by a synthetic flocculant: a polarographic study of the complexation with a high molecular weight poly(acrylic acid) for different pH values. Water Research 34 (2000): 455-462.

[31] CosŸkun, R., Soykan, C. and Sacak, M. Adsorption of copper(II), nickel(II) and cobalt(II) ions from aqueous solution by methacrylic acid/acrylamide monomer mixture grafted poly(ethylene terephthalate) fiber. Separation and Purification Technology 49 (2006): 107-114.

[32] Li, D., Huang, J. and Kaner, R. B. Polyaniline nanofibers: a unique polymer nanostructure for versatile applications. Accounts of Chemical Research 42 (2008): 135-145.

[33] Li, Q., Sun, L., Zhang, Y., Qian, Y. and Zhai, J. Characteristics of equilibrium, kinetics studies for adsorption of Hg(II) and Cr(VI) by polyaniline/humic acid composite. Desalination 266 (2011): 188-194.

[34] Huang, Y. F. and Lin, C. W. Exploration of the formation mechanisms of polyaniline nanotubes and nanofibers through a template-free method. Synthetic Metals 159 (2009): 1824-1830.

[35] Zhang, Z., Wei, Z., Zhang, L. and Wan, M. Polyaniline nanotubes and their dendrites doped with different naphthalene sulfonic acids. Acta Materialia 53 (2005): 1373-1379.

[36] Zhang, L., Peng, H., Sui, J., Kilmartin, P. A. and Travas-Sejdic, J. Polyaniline nanotubes doped with polymeric acids. Current Applied Physics 8 (2008): 312-315.

[37] Ghorbani, M., Lashkenari, M. S. and Eisazadeh, H. Application of polyaniline nanocomposite coated on rice husk ash for removal of Hg(II) from aqueous media. Synthetic Metals 161 (2011): 1430-1433.

[38] Zhang, Y., Li, Q., Sun, L., Tang, R. and Zhai, J. High efficient removal of mercury from aqueous solution by polyaniline/humic acid nanocomposite. Journal of Hazardous Materials 175 (2010): 404-409.

[39] MacDiarmid, A. G. and Epstein, A. J. Polyaniline: synthesis, chemistry and processing. New Aspects of Organic Chemistry II Proceedings of the Fifth International Kyoto Conference (1992).

[40] Palaniappan, S. and John, A. Polyaniline materials by emulsion polymerization pathway. Progress in Polymer Science 33 (2008): 732-758.

[41] Shreepathi, S. Dodecylbenzenesulfonic acid: a surfactant and dopant for the synthesis of processable polyaniline and its copolymer (2006).

[42] Umadevi, G., Ponnusamy, V., M.Paramsivam and Elango, A. Effect of D.C. voltages using HCl for the synthesis and characterization of polyaniline. Portugaliae Electrochimica Acta 26 (2008): 461-467.

[43] Bai, H. and Shi, G. Gas sensors based on conducting polymers. Sensors 7 (2007): 267-307.

[44] Sengupta, P. P. and Adhikari, B. Influence of polymerization condition on the electrical conductivity and gas sensing properties of polyaniline. Materials Science and Engineering: A 459 (2007): 278-285.

[45] R.N. Singh, M. and Awasthi, R. Polypyrrole composites: electrochemical synthesis, characterizations and applications. Electropolymerization (2011): 131-158.

[46] Stejskal, J., Sapurina, I. and Trchova, M. Polyaniline nanostructures and the role of aniline oligomers in their formation. Progress in Polymer Science 35 (2010): 1420-1481.

[47] Pan, L., Qiu, H., Dou, C., Li, Y., Pu, L., Xu, J. and Shi, Y. Conducting polymer nanostructures: template synthesis and applications in energy storage. International journal of molecular sciences 11 (2010): 2636-2657.

[48] Zhang, D. and Wang, Y. Synthesis and applications of one-dimensional nano-structured polyaniline: An overview. Materials Science and Engineering: B 134 (2006): 9-19.

[49] Stejskal, J., Sapurina, I. and Trchovรก, M. Polyaniline nanostructures and the role of aniline oligomers in their formation. Progress in Polymer Science 35 (2010): 1420-1481.

[50] Cao, G. and Liu, D. Template-based synthesis of nanorod, nanowire, and nanotube arrays. Advances in Colloid and Interface Science 136 (2008): 45-64.

[51] Hsieh, B.-Z., Chuang, H.-Y., Chao, L., Li, Y.-J., Huang, Y.-J., Tseng, P.-H., Hsieh, T.-H. and Ho, K.-S. Formation mechanism of a nanotubular polyanilines prepared by an emulsion polymerization without organic solvent. Polymer 49 (2008): 4218-4225.

[52] Laslau, C., Zujovic, Z. D. and Travas-Sejdic, J. Polyaniline "Nanotube" Self-Assembly: The Stage of Granular Agglomeration on Nanorod Templates. Macromolecular Rapid Communications 30 (2009): 1663-1668.

[53] Ding, Z., Currier, R. P., Zhao, Y. and Yang, D. Self-Assembled Polyaniline Nanotubes with Rectangular Cross-Sections. Macromolecular Chemistry and Physics 210 (2009): 1600-1606.

[54] Laslau, C., Zujovic, Z. and Travas-Sejdic, J. Theories of polyaniline nano-structure self-assembly: Towards an expanded, comprehensive Multi-Layer Theory (MLT). Progress in Polymer Science 35 (2010): 1403-1419.

[55] Huang, Y. F. and Lin, C. W. Introduction of methanol in the formation of polyaniline nanotubes in an acid-free aqueous solution through a self-curling process. Polymer 50 (2009): 775-782.

[56] Daley, R. F. and Daley, S. J. Organic chemistry Chapter 5 (2005).

[57] AdiChemistry. Pearson's Hard and Soft Acids and Basas (HSAB) Theory [Online], 16 April 2013, Source http://www.adichemistry.com/inorganic/cochem/hsab/hard-soft-acid-base-theory.html.

[58] Li, G., Pang, S., Xie, G., Wang, Z., Peng, H. and Zhang, Z. Synthesis of radially aligned polyaniline dendrites. Polymer 47 (2006): 1456-1459.

[59] Zhou, S., Wu, T. and Kan, J. Effect of methanol on morphology of polyaniline. European Polymer Journal 43 (2007): 395-402.

[60] Lü, Q.-F., Huang, M.-R. and Li, X.-G. Synthesis and heavy-metal-ion sorption of pure Sulfophenylenediamine copolymer nanoparticles with intrinsic conductivity and stability. Chemistry – A European Journal 13 (2007): 6009-6018.

[61] Jin, L. Mechanisms of lead adsorption on Chitosan/PVA hydrogel beads. Langmuir 18 (2002): 9765-9770.

VITA

Miss Sirinan Khunrit was born on November 1, 1987 in Nakornsithammarat, Thailand. She graduated with a Bachelor of Engineering, Faculty of Engineering and Industrial Technology, Program of Petrochemicals and Polymeric Materials, Silpakorn University in 2010. After that, she has been a graduate student at Program of Petrochemistry and Polymer Science, Faculty of Science, Chulalongkorn University and become a member of Chromatography and Separation Research Unit. She finished her Master's degree of Science in 2013.

Poster presentation and proceeding

"Effect of organic acid dopants on the preparation of polyaniline nanotubes via a self-assembly method" Sirinan Khunrit, Puttaruksa Varanusupakul. Poster presentation and proceeding, *Pure and Applied Chemistry International Conference 2013 (PACCON 2013),* The Tide Resort, Bangsaen Beach, Chonburi, Thailand, 23-25 January, 2013.